THE IMPORTANCE OF LENS GALAXY ENVIRONMENTS

Charles R. Keeton[1]

Astronomy & Astrophysics Department, University of Chicago, 5640 South Ellis Avenue, Chicago, IL 60637

AND

Ann I. Zabludoff

Steward Observatory, University of Arizona, 933 North Cherry Avenue, Tucson, AZ 85721

Received 2004 March 9; accepted 2004 May 20

ABSTRACT

It is suspected that many strong gravitational lens galaxies lie in poor groups or rich clusters of galaxies, which modify the lens potentials. Unfortunately, little is actually known about the environments of most lenses, so environmental effects in lens models are often unconstrained and sometimes ignored. We show that such poor knowledge of environments introduces significant biases and uncertainties into a variety of lensing applications. Specifically, we create a mock poor group of 13 galaxies that resembles real groups, generate a sample of mock lenses associated with each member galaxy, and then analyze the lenses with standard techniques. We find that standard models of two-image (double) lenses, which neglect environment, grossly overestimate both the ellipticity of the lens galaxy ($\Delta e/e \sim 0.5$) and the Hubble constant ($\Delta h/h \sim 0.22$). Standard models of four-image (quad) lenses, which approximate the environment as a tidal shear, recover the ellipticity reasonably well ($|\Delta e/e| \lesssim 0.24$) but overestimate the Hubble constant ($\Delta h/h \sim 0.15$) and have significant ($\sim 30\%$) errors in the millilensing analyses used to constrain the amount of substructure in dark matter halos. For both doubles and quads, standard models slightly overestimate the velocity dispersion of the lens galaxy ($\Delta\sigma/\sigma \sim 0.06$) and underestimate the magnifications of the images ($\Delta\mu/\mu \sim -0.25$). Standard analyses that use the statistics of lens populations to place limits on the dark energy overestimate Ω_Λ (by 0.05–0.14) and underestimate the ratio of quads to doubles (by a factor of 2). The systematic biases related to environment help explain some long-standing puzzles (such as the high observed quad/double ratio) but aggravate others (such as the low value of H_0 inferred from lensing). Most of the biases are caused by neglect of the convergence (gravitational focusing) from the mass associated with the environment, but additional uncertainty is introduced by neglect of higher order terms in the lens potential. Fortunately, we show that directly observing and modeling lens environments should make it possible to remove the biases and reduce the uncertainties. Such sophisticated lensing analyses will require finding the other galaxies that are members of the lensing groups and measuring the group centroids and velocity dispersions, but they should reduce systematic effects associated with environments to the few percent level.

Subject headings: cosmological parameters — dark matter — galaxies: clusters: general — galaxies: halos — gravitational lensing

1. INTRODUCTION

The study of strong gravitational lenses offers unique constraints on the masses and properties of galaxy dark matter halos (e.g., Kochanek 1991; Keeton et al. 1998; Rusin et al. 2003b; Treu & Koopmans 2004), the properties of quasars (e.g., Nemiroff 1988; Richards et al. 2004) and their host galaxies (e.g., Rix et al. 2001; Kochanek et al. 2001; Peng et al. 2004), the Hubble constant (e.g., Refsdal 1964; Kochanek & Schechter 2003), the nature of dark matter (e.g., Metcalf & Madau 2001; Dalal & Kochanek 2002), and the properties of dark energy (e.g., Turner 1990; Kochanek 1996a; Chae 2003; Mitchell et al. 2004; Linder 2004). The number of strong lenses is approaching 100, with useful subsamples that number in the tens (e.g., Browne et al. 2003; Rusin et al. 2003a; Ofek et al. 2003), and will grow dramatically with ongoing and future surveys (e.g., Kuhlen et al. 2004). The relative positions and fluxes of the lensed images are routinely measured to high precision with the *Hubble Space Telescope* and radio interferometers (e.g., Lehár et al. 2000; Patnaik et al. 1999; Trotter et al. 2000); Einstein rings or arcs are proving to be common in high-resolution near-IR images (e.g., Kochanek et al. 2001), and image time delays and lens galaxy velocity dispersions are succumbing to concerted observational effort (e.g., Schechter et al. 1997; Burud et al. 2002a, 2002b; Fassnacht et al. 2002; Colley et al. 2003; Treu & Koopmans 2002a, 2004). With such extensive and high-quality data in hand, the results of lensing analyses are limited mainly by systematic uncertainties in the lens models required to interpret the data.

We are interested in systematic uncertainties related to the fact that lens galaxies are not isolated. Many lenses are produced by early-type galaxies that reside in overdense regions like poor groups or rich clusters of galaxies (e.g., Young et al. 1980; Kundić et al. 1997a, 1997b; Tonry 1998; Tonry & Kochanek 1999; Kneib et al. 2000; Fassnacht & Lubin 2002; I. Momcheva et al. 2004, in preparation; K. Williams et al. 2004, in preparation). The additional mass near the lens contributes both a "convergence" (additional gravitational focusing) and "shear" (gravitational tidal force)[2] to the lens

---

[1] Hubble Fellow.

[2] This shear is formally equivalent to that probed with weak lensing analyses of clusters and cosmic shear (see reviews by Bartelmann & Schneider 2001; van Waerbeke & Mellier 2003), even though it is detected in a different way.

potential, plus higher order terms that may or may not be small (see § 2). One set of systematic uncertainties in lens models occurs because the convergence is degenerate with the lens galaxy mass, in all lens observables but the time delays; this is the well-known "mass-sheet degeneracy" (Gorenstein et al. 1988; Saha 2000). Because of the degeneracy, the convergence is usually omitted from lens models, which leads to a variety of biases. Attempts to correct the biases—for example, by using independent weak lensing analyses to constrain the convergence (e.g., Bernstein & Fischer 1999)—have been rare.

A second set of systematic effects occurs because the shear is approximately degenerate with the ellipticity of the lens galaxy (Keeton et al. 1997). Two-image (double) lenses suffer badly: even when environmental effects are strong, models without shear fit the data just fine, and models that include shear reveal it to be degenerate with ellipticity. Without independent knowledge of the environment, the natural choice for doubles is to omit shear, but that must introduce errors into the models. The situation is better for four-image (quad) lenses, because the degeneracy between ellipticity and shear is only approximate. Both effects produce quadrupole terms in the lens potential, but with different radial dependences: $\phi \propto \gamma r^2 \cos 2(\theta - \theta_\gamma)$ for shear, and $\phi \propto er \cos 2(\theta - \theta_e)$ for ellipticity. Quads generally have enough constraints to detect the difference, and thus to reveal that shear cannot be neglected (e.g., Keeton et al. 1997). Even so, models of quads may not uniquely constrain both the ellipticity and shear, leaving a large range of allowed models. Furthermore, for both doubles and quads we must ask whether approximating the environmental effects as a simple shear (neglecting higher order terms in the lens potential) is adequate.

These issues can be collected into a general question: *If lens galaxy environments are poorly known, how wrong will standard lensing analyses be?* We address the question by placing galaxies in simple but realistic environments whose properties we understand and control, and using them to generate catalogs of mock lenses. We then apply standard lensing analyses to the mock lenses, and study whether the results accurately recover the input parameters. We consider a wide range of astrophysical and cosmological problems to which lensing is applied, including the shapes and masses of galaxy dark matter halos, the amount of substructure in dark matter halos, the properties of lensed sources, the Hubble constant, and the dark energy density. In this paper we begin by examining a single (but typical) case to identify problems that arise when lens environments are unknown. In a subsequent analysis we will study in more detail how the errors depend on the properties of the environment.

We stress that we focus on arcsecond-scale lens systems in which the lens potential is dominated by one galaxy (or occasionally two or three galaxies in close proximity; Rusin et al. 2001; Keeton & Winn 2003), and the contribution from the environment can be treated as a perturbation. This is the case for nearly all multiply-imaged quasars and radio sources. It differs from the case of lensed arcs (e.g., Gladders et al. 2003; Zaritsky & Gonzalez 2003) and wide-separation lensed quasars (e.g., Inada et al. 2003), which are produced by the large dark matter halos of clusters.

In this paper we focus on systematic effects associated with the angular structure of the potential. There is an additional set of systematic effects associated with the fact that in models of many lenses the radial density profile of the lens galaxy is degenerate. We explicitly neglect this degeneracy by always assuming that the galaxies can be modeled as isothermal ellipsoids. This simple assumption seems to be remarkably good (e.g., Zaritsky & White 1994; Rix et al. 1997; Gerhard et al. 2001; McKay et al. 2002; Treu & Koopmans 2002a; Koopmans et al. 2003; Rusin et al. 2003b; Sheldon et al. 2004). Even if this assumption comes into question (see Romanowsky et al. 2003), the crucial point is that we use a fixed radial density profile for both generating and modeling mock lenses. In this way we avoid any systematic errors associated with the radial profile, and highlight systematic effects associated with environment. In the follow-up analysis we will also examine systematics related to the radial profile and consider whether knowledge of lens galaxy environments can actually help break the profile degeneracy. Other recent investigations have studied the radial profile degeneracy in considerable detail (e.g., Treu & Koopmans 2002a, 2002b, 2004; Rusin et al. 2003b).

This paper is organized as follows. We first create a typical lens environment, a poor group of galaxies that mimics the group around the observed lens PG 1115+080 (§ 2). We use the galaxies in the group to create a catalog of mock lenses (§ 3). We then analyze the mock lenses with standard techniques to identify environment-induced uncertainties and biases in a variety of lensing applications (§ 4). Finally, we show how knowledge of the environment can be used to remove the systematic effects (§ 5). We offer some general comments in § 6, and summarize our conclusions in § 7.

2. A MOCK GROUP OF GALAXIES

Although the full distribution of lens galaxy environments is not well known, predictions (Keeton et al. 2000) and observations (e.g., Kundić et al. 1997a, 1997b; Tonry 1998; Tonry & Kochanek 1999; Fassnacht & Lubin 2002; I. Momcheva et al. 2004, in preparation; K. Williams et al. 2004, in preparation) indicate that the most common lens environments are probably poor groups of galaxies. We seek to create a mock group that mimics the group at redshift $z = 0.31$ around the four-image lens PG 1115+080 (Kundić et al. 1997a; Tonry 1998; I. Momcheva et al. 2004, in preparation). This group appears to be typical of lens environments and similar to X-ray selected groups in the nearby universe (Zabludoff & Mulchaey 1998, 2000) in terms of its galaxy population, kinematics, and X-ray properties (Grant et al. 2003; I. Momcheva et al. 2004, in preparation). In addition, this lens is a favorite for many lensing applications (e.g., Schechter et al. 1997; Keeton & Kochanek 1997; Saha & Williams 1997; Impey et al. 1998; Zhao & Pronk 2001; Treu & Koopmans 2002b), so it offers an insightful example.

The lens in PG 1115+080 consists of four images of a quasar at redshift $z_s = 1.72$ around an early-type galaxy at redshift $z_l = 0.31$. Kundić et al. (1997a) and Tonry (1998) discovered that there are four other galaxies at the same redshift spanning $24''$ on the sky and forming a group with velocity dispersion $\sigma \sim 300$ km s^{-1}. I. Momcheva et al. (2004, in preparation) have expanded the group membership to 13 galaxies spanning $4.'5$, and calculated a velocity dispersion of $\sigma = 354 \pm 53$ km s^{-1}. We use the relative positions of these galaxies, together with the relative magnitudes given by K. Williams et al. (2004, in preparation).

In deciding how to distribute the mass within the group, it is useful to consider two extreme cases that bound the possibilities. One case places all of the mass in the group member galaxies and their individual dark matter halos; this could represent a system where the galaxies have not interacted tidally with each other. The other case places all of the mass in a

common dark matter halo, such that the galaxies are essentially massless tracers of the group potential. In nearby groups, the kinematics of group member galaxies and the presence of extended X-ray luminous halos suggest that the most of the mass is in a common group halo (Zabludoff & Mulchaey 1998; Mulchaey & Zabludoff 1998). The situation is less clear for the distant groups ($0.3 \lesssim z \lesssim 1$) where lens galaxies are likely to be found. X-ray halos have been detected in two lensing groups at $z \sim 0.3$ (including PG 1115+080; Grant et al. 2003), but studying them well enough to probe the group mass distributions is exceedingly difficult (the X-ray halos are faint extended sources that have the bright quasar image superposed). Theoretically, one might expect distant groups to be less dynamically evolved than nearby groups and thus to have less mass in a common halo. Given the uncertainties, we have analyzed both of these extreme cases. The systematic errors in lens models are qualitatively quite similar for the two cases, so we present only the case where all of the mass is in the galaxies and their individual dark matter halos. This choice makes it easier to discuss how observations of lens environments can be used to reduce or remove the model errors (see § 5).

We model the galaxies as isothermal ellipsoids, which is consistent with evidence from strong lensing, stellar dynamics, and X-ray studies on small scales (Fabbiano 1989; Rix et al. 1997; Gerhard et al. 2001; Treu & Koopmans 2002a; Koopmans et al. 2003; Rusin et al. 2003b), and with galaxy-galaxy lensing and satellite kinematics on large scales (Zaritsky & White 1994; McKay et al. 2002; Sheldon et al. 2004). An isothermal ellipsoid has projected surface mass density (in units of the critical density for lensing)

$$\kappa = \frac{\Sigma}{\Sigma_{\rm crit}} = \frac{b}{2r}\left[\frac{1+q^2}{(1+q^2)+(1-q^2)\cos 2(\theta-\theta_0)}\right]^{1/2}, \quad (1)$$

where $q \leq 1$ is the axis ratio, θ_0 is the orientation angle (defined as a position angle measured east of north), and b is a mass parameter related to the velocity dispersion σ by

$$b = 4\pi\left(\frac{\sigma}{c}\right)^2\frac{D_{ls}}{D_{os}}, \quad (2)$$

where D_{os} and D_{ls} are angular diameter distances from the observer to the source and from the lens to the source, respectively. For a spherical galaxy b equals the Einstein radius, while for a nonspherical galaxy b and $R_{\rm E}$ differ by no more than a few percent for reasonable axis ratios. The lensing properties of isothermal ellipsoids are given by Kassiola & Kovner (1993), Kormann et al. (1994), and Keeton & Kochanek (1998).

The spectra of group member galaxies indicate that many are early-type galaxies (I. Momcheva et al. 2004, in preparation), so we use the Faber-Jackson relation ($L \propto \sigma^4$) to estimate the galaxies' velocity dispersions and b parameters. Specifically, the ratio of the b parameters for two galaxies i and j is estimated from their relative magnitudes,

$$\frac{b_i}{b_j} = 10^{-0.2(m_i - m_j)}. \quad (3)$$

Scatter in the Faber-Jackson relation (e.g., Sheth et al. 2003) could cause scatter between these b ratios and the actual values for the PG 1115+080 group, but that is irrelevant because we use equation (3) to *define* the mock group. We determine the scale by setting $b = 1\rlap{.}''0$ for the galaxy that is an analog of the lens galaxy in PG 1115+080 (galaxy 1 in Table 1 below); this value is both consistent with the observed lens (Impey et al. 1998) and typical of all lenses (see the image separation distributions in, e.g., Keeton et al. 2000; Kuhlen et al. 2004).

We assign all of the galaxies an ellipticity $e = 1 - q = 0.3$, which is typical for early-type galaxies (e.g., Bender et al. 1989; Saglia et al. 1993; Jørgensen et al. 1995), and we give them random orientations. The resulting parameters for the mock group galaxies are given in Table 1. A visual sense of the group is given in Figure 1. Note that the left panel shows the projected mass (not light) distribution, so it is perhaps more comparable to maps from N-body simulations than to images of observed groups.

It is worth pointing out that even though we study a single global system (the group), each galaxy has a unique local environment so we actually have 13 sample lens galaxy environments. As a further test of whether the group is reasonable,

TABLE 1
PROPERTIES OF THE MOCK GROUP

Galaxy	x (arsec)	y (arcsec)	b (arcsec)	e	θ (deg)	$\kappa_{\rm env}$	$\gamma_{\rm env}$	N_2	N_4
1...............	0.0	0.0	1.00	0.3	60.3	0.1123	0.0950	422	215
2...............	21.3	−11.3	1.38	0.3	85.6	0.1440	0.0859	931	415
3...............	13.1	−1.4	0.87	0.3	−3.3	0.1782	0.1090	419	145
4...............	15.2	−12.4	0.66	0.3	63.9	0.2438	0.0797	293	138
5...............	14.6	−4.3	0.19	0.3	1.5	0.3148	0.2428	11	37
6...............	5.5	−117.4	0.43	0.3	66.4	0.0268	0.0209	70	11
7...............	−38.6	10.4	0.39	0.3	−72.1	0.0626	0.0449	72	17
8...............	−20.2	41.1	0.28	0.3	−34.7	0.0589	0.0439	35	6
9...............	97.9	−19.5	0.51	0.3	9.0	0.0476	0.0382	123	16
10...............	−37.3	81.4	0.27	0.3	28.1	0.0337	0.0300	37	6
11...............	109.4	−29.8	0.41	0.3	11.2	0.0469	0.0388	74	16
12...............	−16.5	9.6	0.35	0.3	11.6	0.0983	0.0814	62	12
13...............	−146.4	−120.5	0.35	0.3	22.7	0.0168	0.0149	57	9

NOTES.—Each galaxy has position (x, y), ellipticity and position angle (e, θ_0), and mass parameter b; and feels a convergence $\kappa_{\rm env}$ and shear $\gamma_{\rm env}$ from its environment; N_2 and N_4 give the number of mock double and quad lenses in our catalog that are associated with each galaxy.
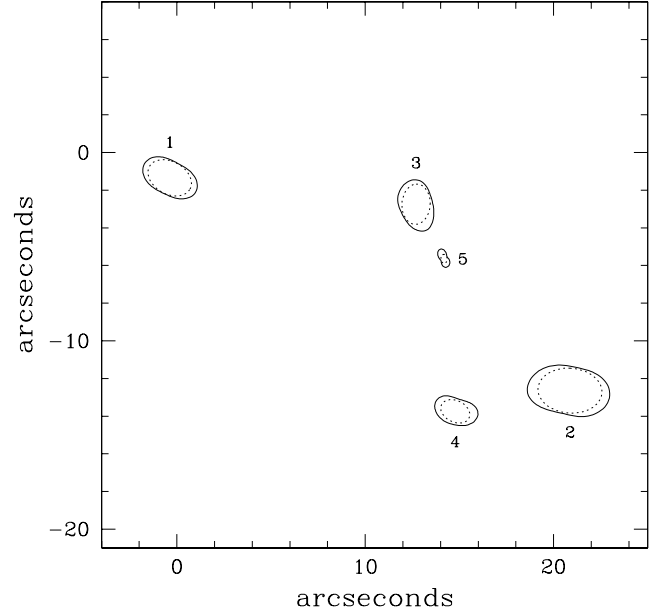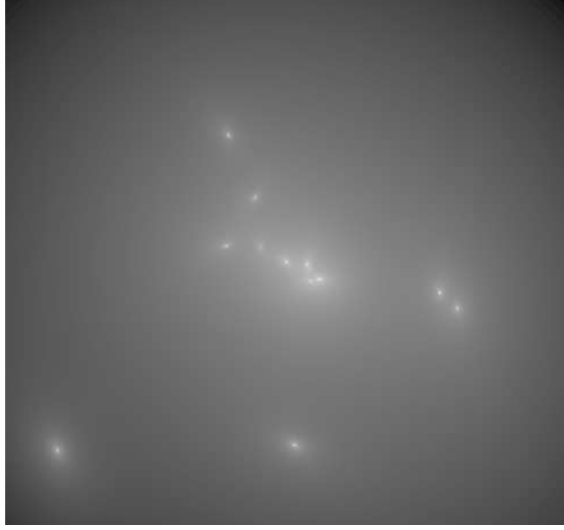
Fig. 1.—*Left*: Logarithmic surface mass density map for the mock group, in the model with all the mass associated with the galaxies and their dark matter halos. The map is $6'$ ($570\ h^{-1}$ kpc) on a side. *Right:* Lensing critical curves in the central region of the group. The solid curves show the actual critical curves; for comparison, the dotted curves show the critical curve each galaxy would have if it were isolated. The galaxies are labeled with the indices from Table 1.

we can quantify the range of environmental contributions to the lens potential. For galaxy i, the environmental piece of the potential is the part due to all the other galaxies:

$$\phi = \phi_i + \phi_{\text{env},i}, \quad \phi_{\text{env},i} \equiv \sum_{j \neq i} \phi_j. \qquad (4)$$

The lensed images tend to lie near a radius (the Einstein radius) that is small compared with the typical distance between galaxies. Therefore we might expand $\phi_{\text{env},i}$ as a Taylor series in polar coordinates centered on galaxy i. The lowest order significant terms are[3]

$$\phi_{\text{env}} = \frac{r^2}{2} \left[\kappa_{\text{env}} + \gamma_{\text{env}} \cos 2(\theta - \theta_\gamma) \right] + \mathcal{O}(r^3), \qquad (5)$$

where κ_{env} and γ_{env} represent, respectively, the convergence (gravitational focusing) and shear (tidal perturbation) discussed in the Introduction. Equivalently, the convergence and shear can be expressed in terms of derivatives of the lens potential (e.g., Schneider et al. 1992):

$$\kappa_{\text{env}} = \frac{1}{2} \left(\frac{\partial^2 \phi_{\text{env}}}{\partial x^2} + \frac{\partial^2 \phi_{\text{env}}}{\partial y^2} \right), \qquad (6)$$

$$\gamma_{\text{env}} = \left(\gamma_{\text{env},+}^2 + \gamma_{\text{env},\times}^2 \right)^{1/2}, \qquad (7)$$

$$\gamma_{\text{env},+} = \frac{1}{2} \left(\frac{\partial^2 \phi_{\text{env}}}{\partial x^2} - \frac{\partial^2 \phi_{\text{env}}}{\partial y^2} \right), \qquad (8)$$

$$\gamma_{\text{env},\times} = \frac{\partial^2 \phi_{\text{env}}}{\partial x \partial y}. \qquad (9)$$

Even if the higher order terms in equation (5) are not negligible, the convergence and shear are still a useful way to quantify the environmental contribution to the lens potential.

Table 1 lists the convergence and shear computed for each galaxy in the mock group, and Figure 2 shows a histogram of the shears. For comparison, Holder & Schechter (2003) have computed the distribution of shears at the positions of early-type galaxies in *N*-body and semianalytic models of galaxy formation. This distribution, which is also shown in Figure 2, represents the range of shears expected in standard galaxy formation models and is also broadly consistent with the shears required to fit observed four-image lenses (see Keeton et al. 1997; Holder & Schechter 2003), so it provides at least a rough guide to the shears felt by real lenses. Although the sample size is small, the shear distribution for our mock group is remarkably similar to the distribution found by Holder &
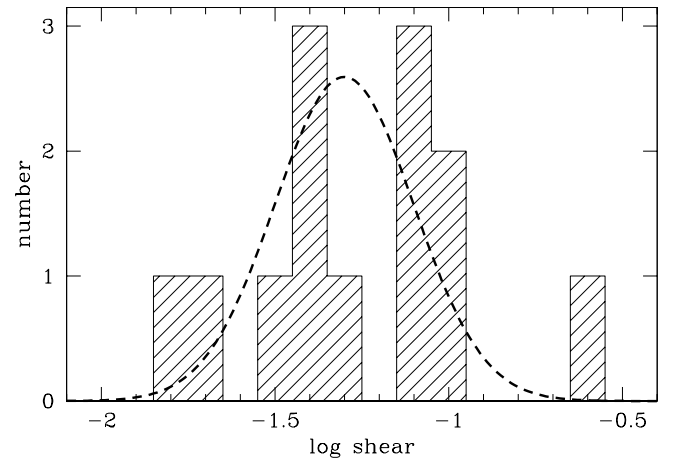

Fig. 2.—Histogram shows the shear distribution for the 13 galaxies in the mock group. The dashed curve shows the distribution for early-type galaxies in galaxy formation simulations (Holder & Schechter 2003).

---

[3] The $\mathcal{O}(r^0)$ term represents the unobservable zero point of the potential, while the $\mathcal{O}(r)$ terms represent an unobservable uniform deflection.

Schechter.[4] While this test is by no means conclusive, it does suggest that our mock group is not way off base and is in fact quite compatible with the expected distribution of environmental contributions to lens potentials.

3. A MOCK LENS CATALOG

3.1. *Basic Approach*

While our mock group represents a single global system, the 13 member galaxies all have different *local* environments and therefore sample the range of environments that may be common to group galaxies. We have already made use of this fact in examining the distribution of shears and using it to argue that our group is reasonable. The next step is to sample the range of lens systems associated with these different environments. We do this by creating a catalog of mock lenses: we place many random sources behind the group, determine which are strongly lensed, and tabulate the positions, magnifications, and time delays of all the lensed images.

We then employ the mock lens catalog to test the effects of environment in two ways. First, we imagine that we have observed the mock lenses, and we fit each one individually with standard mass models to constrain the lens galaxy properties (mass, ellipticity, substructure, etc.) and Hubble constant H_0. Second, we use the statistics of the lens sample to constrain the cosmological constant Ω_Λ and to study the relative numbers of quad and double lenses. The main question is whether or not standard lensing analyses, in which environment is unknown or poorly understood, yield accurate constraints on the various parameters. In essence, we are using a Monte Carlo approach to sample the errors in lensing analyses that are associated with group environments. The remainder of this section is devoted to the details of the Monte Carlo techniques.

3.2. *Application to Individual Lens Systems*

In creating the mock lens catalog, solving the lens equation to find the images of a given source is straightforward using the algorithm and software by Keeton (2001). The only subtleties relate to how the random background sources are selected. To sample lens properties realistically, we must account for "magnification bias," or the fact that highly magnified lens systems are more readily discovered than less magnified systems (e.g., Turner et al. 1984). If we want to mimic real samples, and in particular if we want to avoid undersampling quad lenses, when choosing sources we should give more weight to those with large magnifications. This amounts to applying a nonuniform probability density in the source plane, which has the form

$$p(\boldsymbol{u})\,d\boldsymbol{u} = f(\boldsymbol{u})\frac{N[S_0/\mu(\boldsymbol{u})]}{N(S_0)}\,d\boldsymbol{u}, \qquad (10)$$

where $f(\boldsymbol{u})$ is 1 if a source at position $\boldsymbol{u}$ is multiply-imaged and 0 otherwise, $\mu(\boldsymbol{u})$ is the magnification of a source at that position, $N(S)$ is the number of background sources brighter than flux S, and S_0 is the flux limit of a survey. If the luminosity

function of sources has a power law form, $dN/dS \propto S^{-\nu}$, then the probability density simplifies to

$$p(\boldsymbol{u})d\boldsymbol{u} = f(\boldsymbol{u})\,\mu(\boldsymbol{u})^{\nu-1}\,d\boldsymbol{u}. \qquad (11)$$

Formally, we just draw from this probability density to generate the sample of sources, and then solve the lens equation to obtain the mock lens catalog.

In practice, the probability density equation (11) is quite complicated (because of the lensing caustics, for example), and there is no general algorithm for drawing from a complicated two-dimensional probability density. Fortunately, a simplification is possible. In the special case $\nu = 2$ we can transform the probability density as follows:

$$p(\boldsymbol{u})\,d\boldsymbol{u} = f(\boldsymbol{u})\sum_{i=1}^{N_{\rm img}}\left|\frac{\partial \boldsymbol{x}_i}{\partial \boldsymbol{u}}\right|d\boldsymbol{u} = f(\boldsymbol{x})\,d\boldsymbol{x}, \qquad (12)$$

where $f(\boldsymbol{x})$ is 1 if an image at position $\boldsymbol{x}$ corresponds to a source that is multiply-imaged, and 0 otherwise. The first equality uses the fact that the total magnification is the sum of the magnifications for all the images, and the magnification of image i is $|\partial \boldsymbol{x}_i/\partial \boldsymbol{u}|$ (see, e.g., Schneider et al. 1992). The second equality uses the fact that $|\partial \boldsymbol{x}/\partial \boldsymbol{u}|$ is the Jacobian of the transformation between the source and image planes. While the sum makes the middle expression look complicated, it just ensures that the probability density is carried into every part of the image plane, with no gaps or overlaps.[5] The bottom line is that with $\nu = 2$, the magnification weighting in the source plane corresponds to *uniform* weighting in the image plane. Therefore, what we can do is sample image positions uniformly within the multiply-imaged region of the image plane and then map them back to the source plane to obtain a set of random sources with magnification weighting.

Apart from ease of use, this transformation has one additional advantage and one small drawback. The drawback is that we have had to assume a source luminosity function of the form $dN/dS \propto S^{-2}$; but this is not so different from the luminosity function of sources in the largest existing lens survey (see § 3.3). The practical goal of including magnification bias is to avoid undersampling quad lenses, and for this purpose the $\nu = 2$ luminosity function is perfectly adequate. The fringe benefit of sampling uniformly on the sky is that each galaxy in the group is automatically weighted by its lensing cross section, so massive galaxies contribute the most to our sample of mock lenses just as they would in reality.

In creating the final catalog, choosing the source density represents a compromise between adequate sampling of the range of lens properties and the computational time required for the lens modeling. We find that a sampling density (in the image plane) of 40 arcsec^{-2} yields a total of 2606 doubles and 1043 quads, which seems sufficiently large but still manageable. The number of mock lenses associated with each of the 13 galaxies is given in Table 1. Once we have created the mock lenses, we imagine observing them with the following measurement uncertainties: $0\rlap.{''}003$ in the positions, which is typical of modern data (from Hubble Space Telescope images or radio interferometry) (see Lehár et al. 2000; Patnaik et al.

---

[4] The point in the high-shear tail is galaxy 5, a small galaxy (near the center of Fig. 1) that lies very close to, and is strongly perturbed by, galaxy 3. This galaxy has a small lensing cross section, so even if its shear is unusually large it contributes little to our analysis and does not affect our conclusions.

[5] The way to think about this is that the full source plane maps into the full image plane, and each image position corresponds to a single source.

1999; Trotter et al. 2000); 10% uncertainties in the fluxes; and time delay uncertainties of 2 days, which is somewhat better than much current data (e.g., Schechter et al. 1997; Burud et al. 2002a, 2002b) but achievable with dedicated campaigns (e.g., Fassnacht et al. 2002; Colley et al. 2003).

The mock lenses require that we specify the cosmology and the redshifts of the source and lens. We adopt a cosmology with $\Omega_M = 0.3$, $\Omega_\Lambda = 0.7$, and $h = 0.7$, and we use the lens redshift $z_l = 0.31$ and source redshift $z_s = 1.72$ to mimic PG 1115+080. Note, however, that these particular values only affect the time delays. The time delay between images i and j has the form

$$\Delta t_{ij} = \frac{1 + z_l}{c} \frac{D_{ol} D_{os}}{D_{ls}} \left\{ \left[\phi(\boldsymbol{x}_i) - \phi(\boldsymbol{x}_j) \right] \right.$$
$$\left. - \frac{1}{2} \left[|\nabla \phi(\boldsymbol{x}_i)|^2 - |\nabla \phi(\boldsymbol{x}_j)|^2 \right] \right\}. \quad (13)$$

The term in the braces is expressed in angular units, so the only physical scale (and the only dependence on redshifts and cosmology) appears in the factors out front. Changing the redshifts or the cosmology would rescale all time delays in the same way and would not affect our conclusions.

Once we have the mock lenses, we fit them using the two standard lens models that are usually applied when nothing is known about environment. When a new lens is discovered, the first thing people usually do is fit it with a singular isothermal ellipsoid (SIE).[6] If the fit is poor, the common next step is to add an external shear—to model a possible environmental perturbation using just the γ_{env} term in equation (5). (The higher order terms are dropped for simplicity and because they are thought to be small; the κ_{env} term is dropped because it leads to the mass-sheet degeneracy.) Lenses are occasionally treated with more complex environment models (e.g., Keeton & Kochanek 1997; Bernstein & Fischer 1999; Koopmans et al. 2002; Kneib et al. 2000), but those models are customized to detailed observational data on the environments. Our goal is to identify the kinds of problems that arise from standard analyses when little or nothing is known about lens environments.

3.3. Application to Lens Statistics

For studying the statistics of lens samples, it is useful to make two small modifications to the mock lens catalog. First, in this analysis we are not limited by the computational effort of modeling the lenses; all we want to do is generate the catalog and then determine its statistical properties. We can therefore increase the sampling density to $\sim 10^5$ arcsec^{-2} to improve the precision of the Monte Carlo calculations.

The second modification relates to magnification bias. We would like to mimic the largest existing lens survey, the Cosmic Lens All-Sky Survey (CLASS; Browne et al. 2003). The luminosity function of sources in CLASS is well described as a power law $dN/dS \propto S^{-\nu}$ with $\nu = 2.1$ (Rusin & Tegmark 2001; Chae 2003). This is sufficiently similar to $\nu = 2$ to justify the simplifying transformation used in § 3.2

(see eq. [12]). However, since we are modifying the catalog for the statistical analysis anyway, we go ahead and use $\nu = 2.1$ to allow a more direct comparison with CLASS.[7]

The first statistical step is to sum over the sources associated with a particular galaxy to obtain that galaxy's lensing cross section. In fact, the quantity of interest is the product of the lensing cross section and the magnification bias, which we term the "biased cross section," and which can be written as

$$\tilde{\sigma} = \int_{mult} \frac{N[S_0/\mu(\boldsymbol{u})]}{N(S_0)} \, d\boldsymbol{u}, \quad (14)$$

where the integral extends over the multiply-imaged region of the source plane and $N(S)$ is again the number of sources brighter than flux S. For a power-law source luminosity function $dN/dS \propto S^{-\nu}$, equation (14) simplifies to

$$\tilde{\sigma} = \int_{mult} \mu(\boldsymbol{u})^{\nu-1} \, d\boldsymbol{u}. \quad (15)$$

By integrating over the full multiply-imaged region behind a galaxy, we obtain the total biased cross section. With similar integrals restricted to the doubly-imaged and quadruply-imaged regions, we can compute the biased cross sections for double and quad lenses separately.

The next statistical step is to sum over galaxies to compute the lensing optical depth τ, which represents the total probability that a given source is lensed. In general, we would consider some appropriate population of galaxies described by a mass function dn/dM (e.g., Turner et al. 1984; Kochanek 1993a):

$$\tau = \frac{1}{4\pi} \int dV \int dM \frac{dn}{dM} \tilde{\sigma}, \quad (16)$$

where the first integral is over the volume between the observer and the source. Replacing $\tilde{\sigma}$ with the biased cross section for doubles or quads, we can compute the optical depths τ_2 and τ_4 for two-image and four-image lenses. The predicted ratio of quad to double lenses is then simply τ_4/τ_2. In practice, we have only 13 discrete galaxies, so we replace the mass integral $\int (dn/dM) \, dM$ with a sum over the group galaxies. Also, we know the group redshift, so we drop the volume integral.

To understand how the optical depth is used to place constraints on Ω_Λ, consider a flat universe with a nonevolving population of lens galaxies. While this simple assumption appears to be surprisingly good (Schade et al. 1999; Im et al. 2002; Ofek et al. 2003; Chae & Mao 2003), allowing some evolution would change some quantitative details but not affect the thrust of our argument (see Mitchell et al. 2004). In the nonevolving case the optical depth takes the form

$$\tau(z_s) = \tilde{\sigma} \Gamma n_{tot} D(z_s)^3, \quad (17)$$

where n_{tot} is the integrated comoving number density of galaxies, Γ is a dimensionless number that depends on the shape of the mass function (see, e.g., Kochanek 1993a; Mitchell et al. 2004), and $D(z)$ is the comoving distance to redshift z. In other words, the optical depth is proportional to the volume of

---

[6] Saha & Williams (1997, 2004) have introduced general nonparametric lens models that do not require the isothermal assumption, or indeed any other explicit assumptions about the lens galaxy mass distribution. However, those models treat the environment as a simple shear, so they are still subject to all of the systematic effects that we identify.

[7] Using $\nu = 2.1$ prevents us from repeating the coordinate transformation used in § 3.2; so we select points uniformly in the source plane and apply the magnification weighting a posteriori, as indicated by eq. (15).
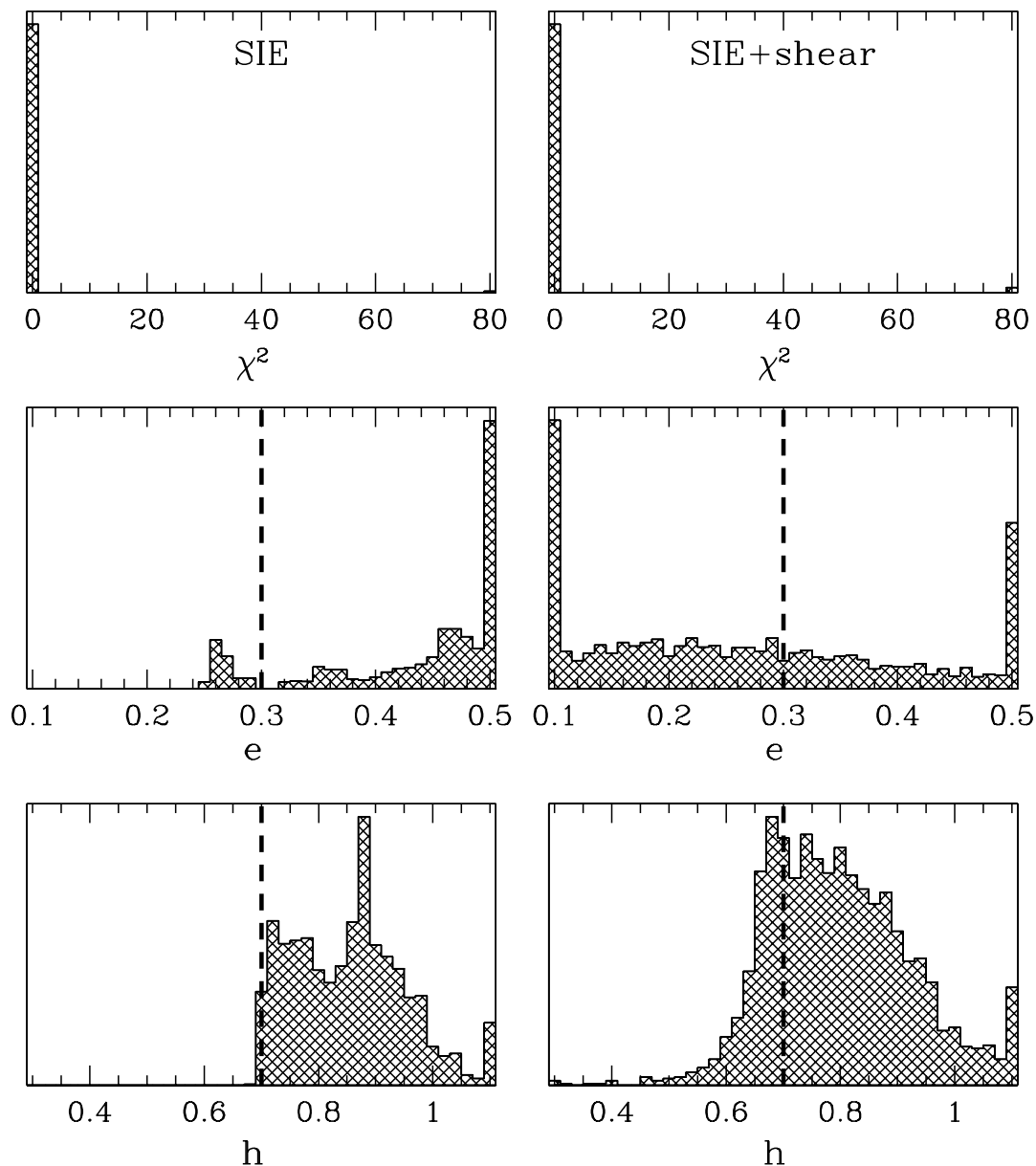
FIG. 3.—Results for models of mock double lenses. SIE models are shown in the left column, and SIE+shear models in the right. The panels show histograms of χ^2 values (*top*), the inferred lens galaxy ellipticity (*middle*), and the Hubble constant (*bottom*). (Note that all values outside the x-axis range are placed in the left- and rightmost bins.) The input values $e = 0.3$ and $h = 0.7$ are indicated by dashed lines.

the universe out to the redshift of the sources. Conceptually, one takes a measurement of the optical depth, adds data or models for the mass function and a model for the cross section, and uses equation (17) to place constraints on the volume of the universe and hence Ω_Λ.

4. IDENTIFYING THE PROBLEMS

4.1. Basic Results: χ^2, e, and h

We first consider some of the basic quantities derived from models of individual lenses: the goodness of fit χ^2, the mass ellipticity e, and the Hubble parameter h. Figure 3 shows histograms of these quantities for SIE and SIE+shear models of the mock double lenses in the catalog from § 3.2. Doubles provide just seven observables: position, and flux for each image, and the time delay. SIE models have seven parameters: b, e, and θ_0 for the galaxy, position and flux for the source,

and h. SIE models of doubles therefore have $N_{\rm dof} = 0$, and in general it is possible to find models that fit the data perfectly ($\chi^2 = 0$). Unfortunately, there are large errors in the recovered mass ellipticity and Hubble parameter caused by the neglect of environment. The problem is worse with SIE+shear models; even though environment is included (in the shear approximation), it is completely unconstrained and so there are enormous uncertainties in the models. *Doubles suffer a fundamental problem: with so few constraints, lens models cannot even detect an environmental component in the lens potential, much less constrain it well enough to yield accurate results.*

Figure 4 shows that the situation is better with quad lenses because the additional images provide more constraints. Quads offer 15 observables: position and flux for each image, and three independent time delays. So both SIE models (seven parameters) and SIE+shear models (nine parameters) are well
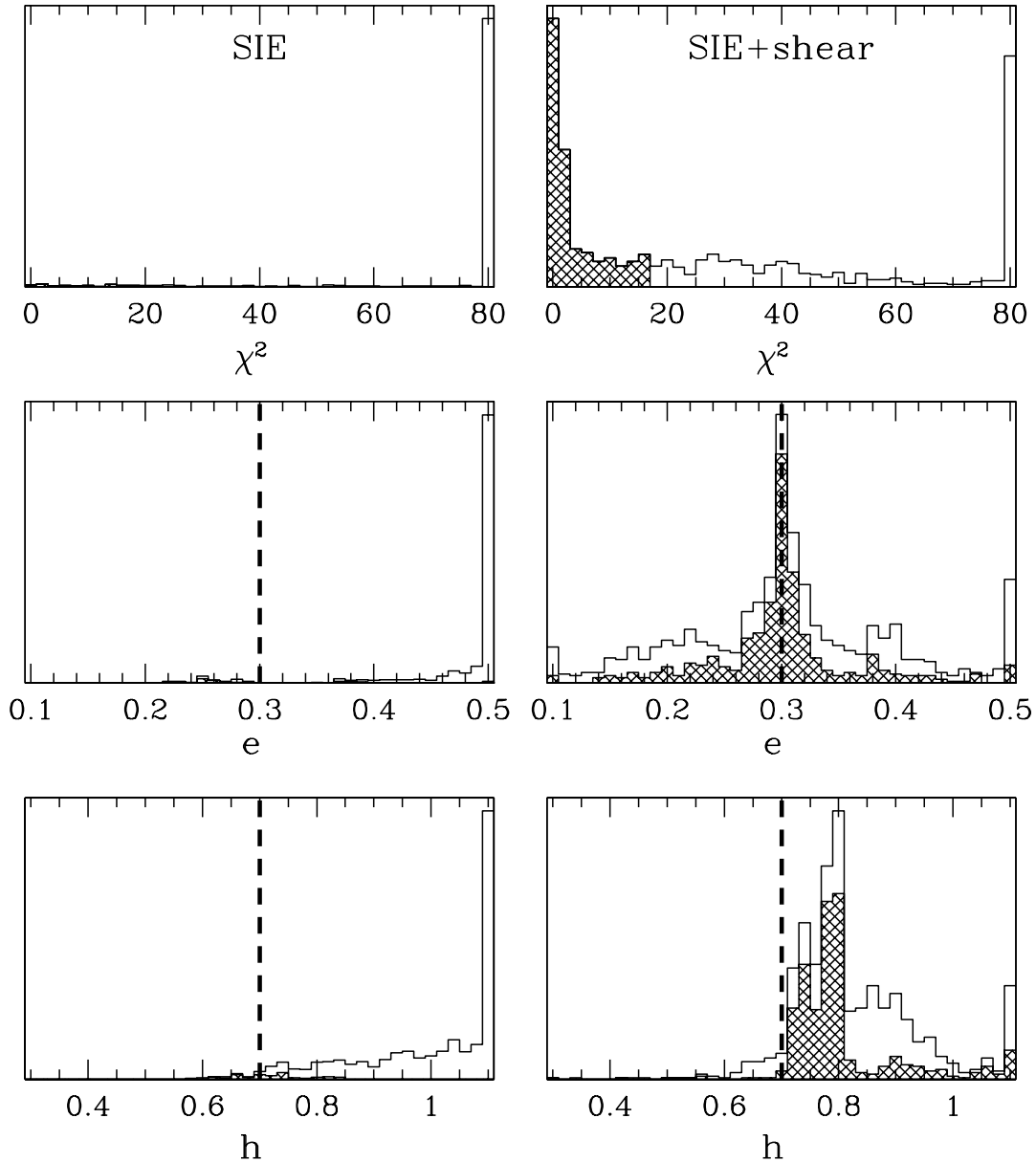
Fig. 4.—Similar to Fig. 3, but for mock quad lenses. The open histograms show all quads, while the shaded histograms show only those where the lens model provides an acceptable fit to the data (models that are not ruled out at the 99% confidence level; see text).

constrained. In fact, SIE models generally give terrible fits: among our mock quads the median χ^2 is 464, and in 95% of the lenses the model can be ruled out at more than 99% confidence ($\chi^2 > 20.1$ for $N_{\mathrm{dof}} = 8$). In other words, quads have enough constraints to make it obvious that environment cannot be neglected. In this case the significant errors in e and h are irrelevant because the χ^2 already reveals that the models are wrong. Like real lenses (Keeton et al. 1997), our mock lenses indicate that quads cannot be well fit by models that neglect environment.

The SIE+shear models of quads are more interesting. Now the median χ^2 among the mock quads is 19.3, and in only 52% of the systems can the model be excluded at 99% confidence ($\chi^2 > 16.8$ for $N_{\mathrm{dof}} = 6$). In the other 48% the SIE+shear model provides an acceptable fit to the data. Thus, approximating the environment as a shear is sufficient to provide a good fit to many quads. *This approximation is not adequate, however, for recovering accurate values for the ellipticity*

and Hubble parameter. The errors in these quantities, while smaller than for doubles, are still worrisome.

Particularly troubling is the fact that the errors are not random but biased. For doubles, SIE models usually overestimate both e and h: the median recovered ellipticity is $e = 0.47$; and (99, 66, 30, 7)% of the mock doubles yield $h > (0.7, 0.8, 0.9, 1.0)$. For quads, SIE+shear models do reasonably well with ellipticity: 88% of the quads with acceptable fits (and 74% of all quads) have ellipticity errors $|\Delta e| < 0.1$. But h is still a problem, as (98, 26, 14, 7)% of the quads with acceptable fits yield $h > (0.7, 0.8, 0.9, 1.0)$. Poor knowledge of environment can clearly cause not just uncertainties but also significant biases in lensing measurements of ellipticity and H_0.

In the remainder of the paper we use the SIE lens models for double lenses (because they give perfect fits, and SIE+shear models are underconstrained), and the SIE+shear models for quads.
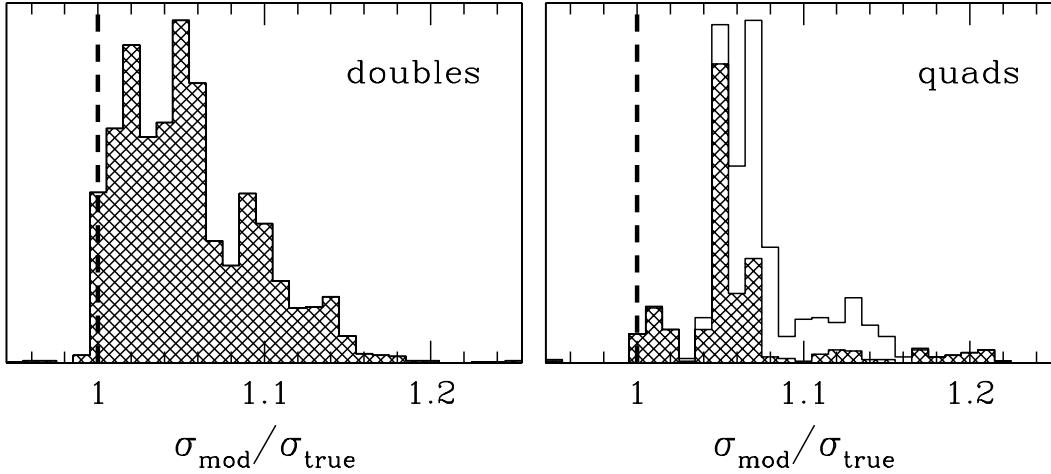
Fig. 5.—Errors in the velocity dispersion of the lens galaxy; σ_{true} is the true (input) value, while σ_{mod} is the value inferred from lens models. The left panel shows doubles; the right panel shows quads, where the open histogram show all quads, while the shaded histograms show only those where the model fits the data. The dashed lines shows where the ratio is unity.

4.2. *Mass and Velocity Dispersion of the Lens Galaxy*

It is often said that lensing robustly measures the mass of the lens galaxy within the Einstein radius. To be precise, this statement applies to quad and Einstein ring lenses, while for doubles lensing measures a mass-radius relation of the form $M(R_1)/R_1 + M(R_2)/R_2 = \pi\Sigma_{\text{crit}}(R_1 + R_2)$, where R_1 and R_2 are the image radii and $M(R)$ is the aperture mass (see Rusin et al. 2003b for a detailed discussion). (Quads and rings can actually be thought of in the same way, but with $R_1 = R_2 = R_E$ since all the images appear near the Einstein radius.) For simplicity we limit our discussion to the mass within the Einstein radius as appropriate for quads and rings, keeping in mind that it would be modified slightly for doubles.

An important caveat is that lensing measures only the total projected mass within the Einstein radius. The total certainly includes contributions from the lens galaxy (its stellar component and dark matter halo). But there is also a contribution of $\pi R_E^2 \kappa_{\text{env}} \Sigma_{\text{crit}}$ from the convergence. Physically, this mass might represent a smooth background in which the galaxy is embedded, such as a common group dark matter halo; or it might represent mass in the immediate foreground or background, such as the halos of other group member galaxies that overlap the line of sight. Models that neglect convergence assume that all of the measured mass must come from the lens galaxy and hence overestimate the galaxy mass.

To examine this effect, it is more instructive to quote the velocity dispersion of the lens galaxy; while the mass depends strongly on the aperture and is not directly observable, the velocity dispersion depends only weakly on aperture (not at all for isothermal models) and is observable (actually the velocity dispersion of the stars; see below). For isothermal models, the mass within the Einstein radius is $M \propto bR_E \propto \sigma^2 R_E$ (see eq. [2]), so the conversion is simple. Figure 5 shows that the models do slightly overestimate the velocity dispersion, with a typical error of $\sim 6\%$ (and a broad range, especially for doubles). While small, the errors are larger than the typical $\sim 1\%$ measurement uncertainties (see Rusin et al. 2003b), and they represent a systematic shift rather than random errors.

The errors may bear on a historic controversy in lensing analyses: the relation between the velocity dispersion of the dark matter (the σ parameter in isothermal models) and that of the stars. Gott (1977) argued that the ratio should be

$\sigma_{\text{DM}}/\sigma_{\text{stars}} = (3/2)^{1/2}$ if galaxy luminosity densities are r^{-3} power laws, but studies of more realistic models for the luminosity indicated that the *central* stellar velocity dispersion σ_0 actually obeys $\sigma_{\text{DM}}/\sigma_0 \approx 1$ (Franx 1993; Kochanek 1993b, 1994). The difference may seem small in the velocity dispersion, but it looms large in lens statistics because the lensing optical depth scales as $\tau \propto \sigma_{\text{DM}}^4$. Most recently, Treu & Koopmans (2004) have found $\langle \sigma_{\text{DM}}/\sigma_0 \rangle = 1.15 \pm 0.05$ by combining direct measurements of σ_0 for five lens galaxies with model determinations of σ_{DM}. We cannot measure this ratio in our simulations since we do not include a stellar component. However, we can say that if standard models are overestimating σ_{DM} then this effect could explain part but not all of the difference of the measured value from unity.

4.3. *Image Magnifications*

In some applications lensing is used as a natural telescope that provides high resolution for studying the structure of quasars and their host galaxies (e.g., Rix et al. 2001; Kochanek et al. 2001; Peng et al. 2004; Richards et al. 2004). In this case accurate lens models are essential for "de-lensing" the system, or removing the effects of lensing magnification and distortion to infer the intrinsic properties of the source. In other applications the need to know the magnification and distortion is less obvious but no less important (see § 4.4). We consider how reliable lens models are for such applications, focusing on the magnifications of unresolved images since we use only pointlike sources.

When studying magnifications it is important to separate images of different types: images that lie at minima of the time delay surface and have positive parity, as opposed to images that lie at saddle points of the time delay surface and are parity-reversed (see, e.g., Schneider et al. 1992). A double has one minimum and one saddlepoint, while a quad has two of each. The image type has become particularly important in studies of microlensing and millilensing (see § 4.4). If the lensed images are pointlike then the parities cannot be observed directly, but image parities can almost always be determined unambiguously with even simple lens models (e.g., Saha & Williams 2003).

Figures 6 and 7 show histograms of the error in the lensing magnification, for doubles and quads respectively. *We see that*
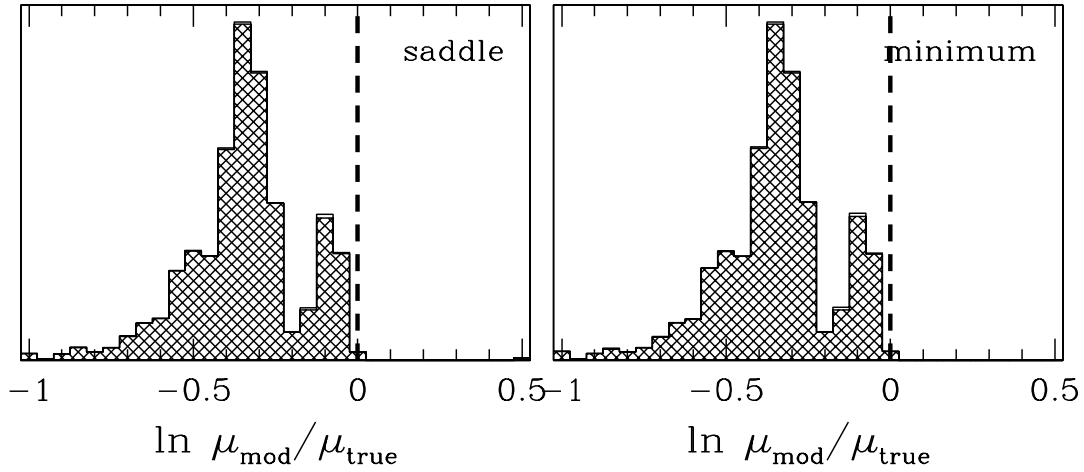
FIG. 6.—Histograms of the ratio of the lensing magnification inferred from lens models to the true magnification, for mock double lenses. The panels refer to the two image classes (saddle points and minima). The dashed lines show where the ratio is unity.

standard lens models tend to underestimate the magnifications, often by a factor of ~ 1.5–2 and sometimes much more. The important qualitative point is that the errors are biased: the models almost always underestimate the magnifications.

4.4. Constraints on Small-Scale Structure

Lensing offers unique constraints on small-scale structure in lens galaxies via the phenomena of microlensing by stars (e.g., Chang & Refsdal 1979; Paczyński 1986; Schmidt & Wambsganss 1998; Wyithe et al. 2000) and millilensing by dark matter clumps (e.g., Mao & Schneider 1998; Metcalf & Madau 2001; Chiba 2002; Dalal & Kochanek 2002). The question is whether environment-related errors in lens models can affect the results. The millilensing constraints, in particular, are derived from lenses with "flux ratio anomalies," or flux ratios that are inconsistent with smooth lens potentials. Conceptually, the probability of having a flux ratio anomaly is given by the abundance of mass clumps times the cross section for any given clump to cause millilensing (to significantly perturb the flux of an image). Converting the abundance of
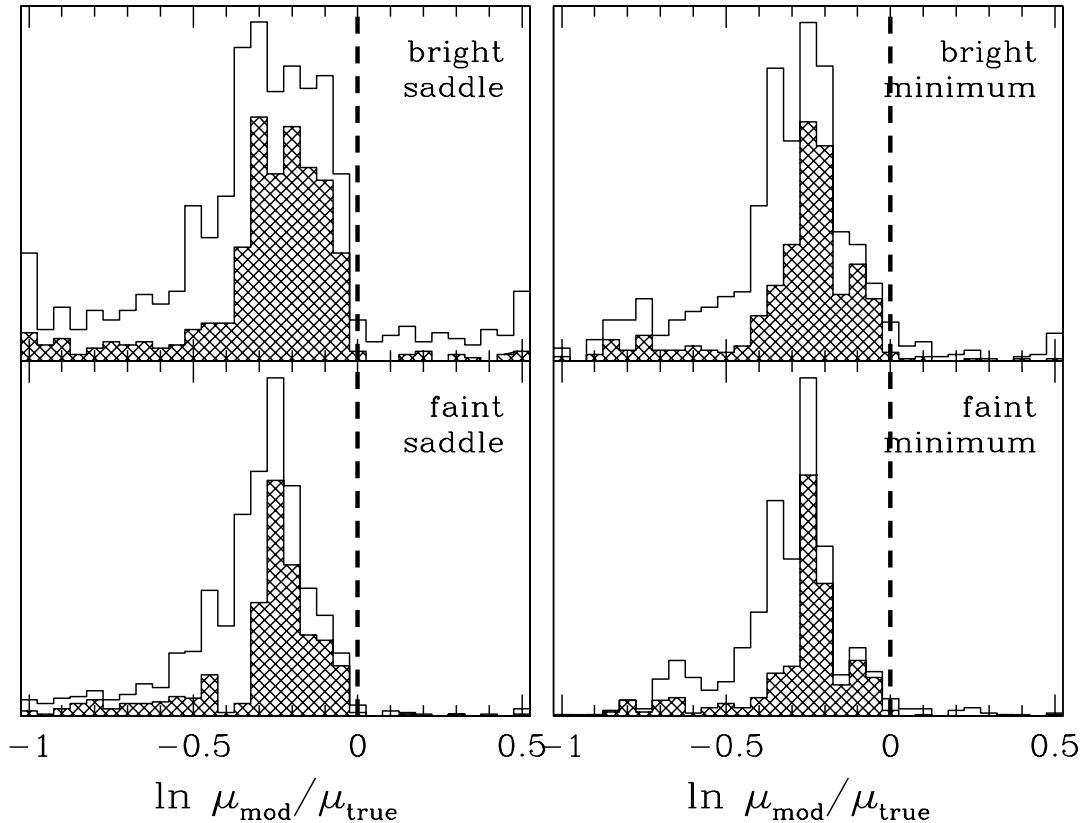

FIG. 7.—Similar to Fig. 6, but for mock quad lenses. The panels refer to the four image classes. The open histograms show all quads, while the shaded histograms show only those where the lens model provides an acceptable fit to the data.
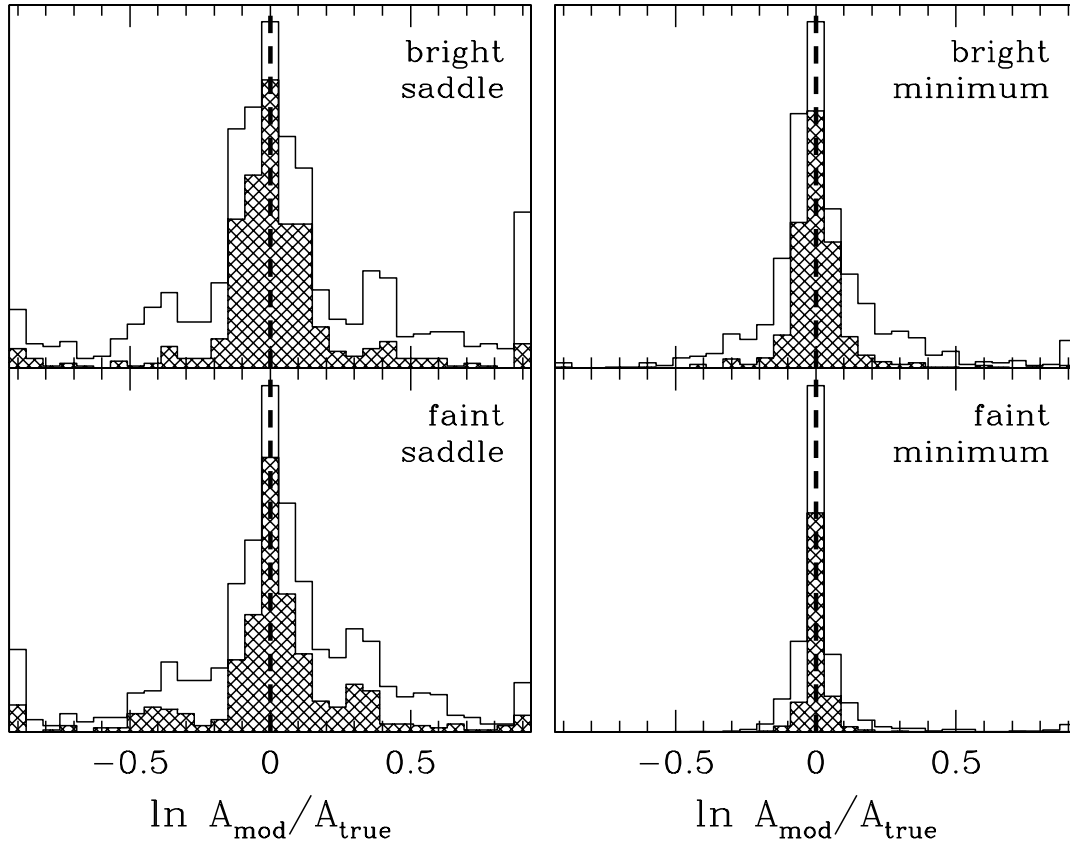
Fig. 8.—Errors in the estimated cross section for millilensing by a mass clump in front of an image in a mock quad lens. The histograms show the ratio of the cross section computed with the fitted lens model to that computed with the true lens potential. The dashed lines show where the ratio is unity. The open histograms show all quads, while the shaded histograms show only those where the lens model provides an acceptable fit to the data.

flux ratio anomalies to a clump abundance therefore requires the ability to compute a clump's millilensing cross section. But that cross section depends in a complicated way on the total lens potential. The dependence is not apparent in the detailed simulations used by Dalal & Kochanek (2002) and Metcalf et al. (2004) to derive clump abundances, but it is made explicit in the analytic expressions derived by Keeton (2003) for the millilensing cross sections of clumps modeled as isothermal spheres.

We focus on millilensing because there are as yet no simple expressions for microlensing cross sections. We compute the cross section for an isothermal clump to produce a 30% change in the flux of an image. Figure 8 shows the ratio of the cross section computed with an SIE+shear lens model to the cross section computed with the true lens potential, for the mock quad lenses.[8] Studying the four types of images separately is important because saddlepoint images—especially the bright saddles—are believed to be particularly susceptible to perturbations; this effect provides a unique signature of lensing by small-scale structure that allows it to be distinguished from other effects (Schechter & Wambsganss 2002; Kochanek & Dalal 2003).

There are indeed errors in the millilensing cross sections due to errors in the lens models. Interestingly, the error distributions appear to be symmetric in $\ln(A_{mod}/A_{true})$. They tend

to have relatively tight cores but broad wings, so the rms error in $\ln(A_{mod}/A_{true})$ is 0.29 for the bright saddles, 0.31 for the faint saddles, 0.14 for the bright minima, and 0.09 for the faint minima. (We are considering only quads where the SIE+shear model provides an acceptable fit.) The fact that bright saddle-point images are so sensitive to the model errors is troubling because they are so important for millilensing analyses.

One would naively expect that a ∼30% uncertainty in the millilensing cross section might cause a comparable uncertainty in the inferred clump abundance, which would make this effect smaller than other statistical and systematic uncertainties in current results (see Dalal & Kochanek 2002). However, to make that statement quantitative and precise we would need to replicate complete millilensing analyses (following, e.g., Dalal & Kochanek 2002; Metcalf et al. 2004). As for microlensing, without a simple way to compute perturbation cross sections we can only guess that there would be qualitatively similar results. Clearly there is much more to do here; we just want to point out that analyses of small-scale structure depend on the overall lens model, and errors in that model related to environment cannot be ignored.

4.5. Constraints on Ω_Λ

We now switch gears and turn to statistical analyses of lens populations and the constraints they yield on the cosmological constant Ω_Λ. As discussed in § 3.3 (see eq. [17]), lensing limits on Ω_Λ depend on the optical depth τ, so the key question is whether environment causes errors in τ. First, though, it is useful to ask whether there are errors in the lensing cross

---

[8] Small-scale structure analyses are usually restricted to quads, because doubles have too few constraints to allow robust identification of flux ratio anomalies.
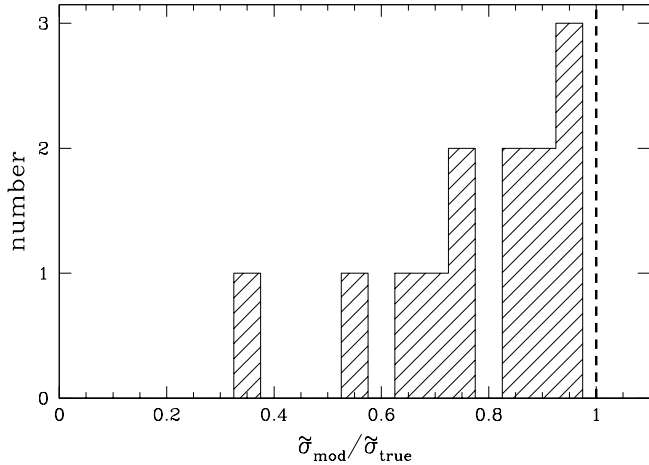
Fig. 9.—Histogram of errors in the lensing cross section; $\tilde{\sigma}_{\mathrm{mod}}$ is the biased cross section with the galaxy assumed to be isolated, while $\tilde{\sigma}_{\mathrm{true}}$ is the value with the galaxy in its proper environment.

Fig. 10.—Errors in the inferred value of Ω_Λ, assuming a typical source redshift $z_s \sim 1.27$ as appropriate for CLASS (Marlow et al. 2000; Chae 2003). The histogram shows the values for the 13 galaxies taken separately. The dashed line shows the input value $\Omega_\Lambda = 0.7$. The arrow at $\Omega_\Lambda = 0.84$ shows the value if we average over the 13 galaxies (weighting each by its cross section). The arrow at $\Omega_\Lambda = 0.75$ shows the value if we assume that 25% of all lens galaxies lie in groups like our mock group, while the other 75% are isolated.

section (from which the optical depth is determined). To answer this question, we compare the biased cross section $\tilde{\sigma}_{\mathrm{true}}$ that a galaxy has when placed in its proper environment to the biased cross section $\tilde{\sigma}_{\mathrm{mod}}$ the *same* galaxy would have if it were assumed to be isolated. Any differences indicate that neglecting environment does cause errors in the cross section. Figure 9 shows the errors in the form of a histogram of the ratio $\tilde{\sigma}_{\mathrm{mod}}/\tilde{\sigma}_{\mathrm{true}}$. *Models that neglect environment underestimate the cross section by tens of percent or more.* The underestimate is caused entirely by the magnification bias,[9] and arises because standard models underestimate the magnifications (see § 4.3).

The next question is how errors in the cross section propagate into errors in Ω_Λ. Figure 10 gives a sense of the effect, by showing the error in Ω_Λ that would result from each of the cross section errors in Figure 9. *Underestimates in the cross sections lead directly to overestimates in Ω_Λ, which can be quite large.* This figure is a bit unfair, because constraints on Ω_Λ properly depend on the optical depth, and not all galaxies contribute equally. For example, the point at $\Omega_\Lambda \approx 1$ (corresponding to the point with $\tilde{\sigma}_{\mathrm{mod}}/\tilde{\sigma}_{\mathrm{true}} = 0.36$ in Fig. 9) is produced by galaxy 5, which is strongly perturbed by galaxy 3. However, galaxy 5 has a small cross section and contributes little to any lens sample, so its properties are not very important. A better approach is to compute the optical depth by summing the cross sections and then compare the "model" (galaxies assumed to be isolated) and true optical depths. This lead to an error $\tau_{\mathrm{mod}}/\tau_{\mathrm{true}} = 0.70$ and hence an inferred value $\Omega_\Lambda = 0.84$ (indicated by an arrow in Figure 10).

This result holds if all lens galaxies lie in environments like our mock group, which is unlikely. The final effect of environment on lens statistics cannot be determined because the distribution of lens galaxy environments is unknown. Still, we can make a crude estimate. Keeton et al. (2000) use galaxy demographics to predict that at least $\sim 25\%$ of lens galaxies lie in groups or clusters. If we conservatively assume that the fraction of lenses with groups is indeed 25%, while the
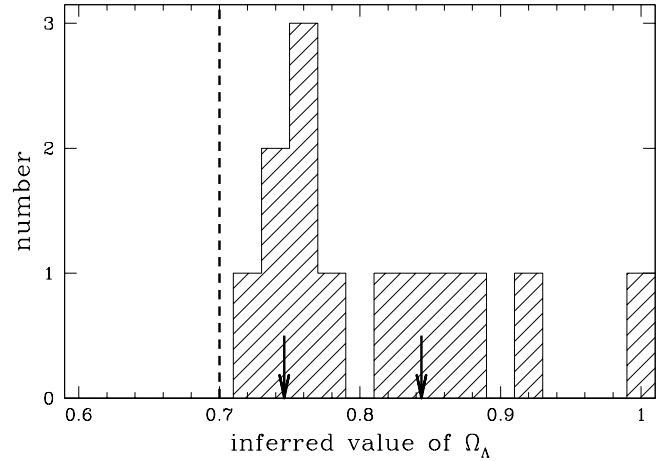
other 75% are isolated, we would find a cross section error $\tau_{\mathrm{mod}}/\tau_{\mathrm{true}} = 0.90$ and hence an inferred value $\Omega_\Lambda = 0.75$ (also indicated in Fig. 10). Even this simple and conservative estimate points to the importance of measuring lens galaxy environments and understanding their effects on lens statistics.

4.6. *The Quad/Double Ratio*

A long-standing puzzle in lens statistics is why so many lenses are quads rather than doubles (King et al. 1996; Kochanek 1996b; Keeton et al. 1997; Rusin & Tegmark 2001; Cohn & Kochanek 2004). In the CLASS statistical sample of 13 lenses, seven are doubles and five are quads (Browne et al. 2003). (The remaining lens is a complicated system that has six images because there are three lens galaxies; see Rusin et al. 2001.) The quad/double ratio depends on the relative cross sections for four- and two-image lenses (along with magnification bias), and it is thought to depend mainly on the ellipticity of lens galaxies. An observed quad/double ratio near unity is said to require a typical ellipticity $e \sim 0.6$ that is much larger than observed or predicted for normal galaxies (Kochanek 1996b; Keeton et al. 1997; Rusin & Tegmark 2001). In fact, some have spoken of the high observed ratio creating an "ellipticity crisis" in lensing (see Kochanek 1996b).

Conventional wisdom holds that environment has little effect on the quad/double ratio, because (when averaged over orientation) shear does not significantly change the two- and four-image cross sections (e.g., Rusin & Tegmark 2001). However, Cohn & Kochanek (2004) recently showed that low-mass satellites around lens galaxies, which are common and not very sensitive to the larger environment, can roughly double the predicted quad/double ratio. We can now determine the effects of a larger group environment, using a model that is more realistic than simple shear.

Under the standard assumption that galaxies are isolated, we would compute a quad/double ratio of 0.25 for each of our galaxies (the same because they all have the same ellipticity). By contrast, placing the galaxies in their proper environments yields the quad/double ratios shown in Figure 11. We find that neglecting environment causes significant errors in the

---

[9] Curiously, the radial caustic of an isothermal lens is not affected by convergence and shear from the environment; the radial caustic is the set of points that map to the origin, and the deflection from convergence and shear vanishes at the origin (see eq. [5]). Except in the rare case of naked cusps, the unbiased cross section is simply the area enclosed by the radial caustic, so it is insensitive to convergence and shear.
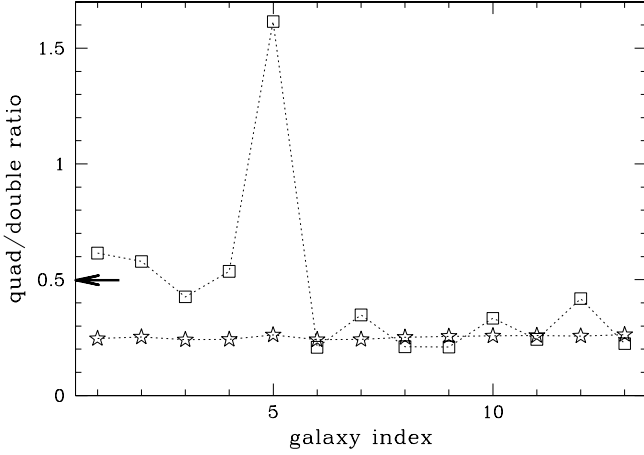
FIG. 11.—Quad/double ratios for the 13 galaxies, computed as the ratio of the biased cross section for four-image lenses to that for two-image lenses. The stars show the results with each galaxy assumed to be isolated; the galaxies should have the same quad/double ratio since they have the same ellipticity, so the fluctuations indicate the level of numerical noise (∼3%). The squares show the results with each galaxy placed in its proper environment. (The lines are drawn just to guide the eye.) The arrow at $Q/D = 0.50$ shows the net ratio when all the galaxy cross sections are summed.

quad/double ratio. More relevant than the individual ratios is the net ratio after summing the two- and four-image cross sections for all the galaxies; this represents the ratio that would be expected for a real lens survey. The net quad/double ratio is again 0.25 when environment is ignored, but 0.50 when environment is included. *In other words, neglecting environment causes a significant underestimate of the quad/double ratio.*

Note that our predicted quad/double ratio of 0.50 is higher than the ratio $1043/2606 = 0.40$ in our mock lenses. Part of the difference may be due to statistical fluctuations in the mock lens catalog, because some of the galaxies produce a small number of lenses (see Table 1). However, most of the difference arises from magnification bias. The mock lenses were generated using magnification bias corresponding to a source luminosity function $dN/dS \propto S^{-\nu}$ with $\nu = 2$ (see § 3). By contrast, the lens statistics calculations use a slightly steeper source luminosity function with $\nu = -2.1$ (as appropriate for comparison to CLASS). The steeper luminosity function produces a larger magnification bias that increases the weight of quads relative to doubles.

Even with environment included our predicted quad/double ratio is still somewhat smaller than observed. Part of the explanation may be that we have assumed a particular ellipticity, $e = 0.3$. Increasing the ellipticity to $e = 0.4$ but holding everything else fixed would yield a quad/double ratio of 0.67 with environment included, which is close to the observed ratio. (With $e = 0.4$ and environment omitted, the quad/double ratio would be 0.40.) A proper analysis would have to include an appropriate distribution of ellipticities. Another part of the explanation may be that we have considered just one mock group, and the full distribution of lens environments will need to be taken into account. A third issue is that we have not considered low-mass satellite galaxies, which would further increase the quad/double ratio (Cohn & Kochanek 2004). Still a fourth possibility is that the high observed quad/double ratio is a statistical fluke. Thorough study of these possibilities is beyond the scope of this paper. We mainly want to point out that environment represents a systematic effect that can significantly increase the predicted quad/double ratio

without violating other constraints (see Rusin & Tegmark 2001).

5. FIXING THE PROBLEMS

Having identified some of the environment-related problems in lensing analyses, we briefly consider what causes them and how they can be fixed. (A fuller treatment of these issues will be given in the follow-up paper.) For doubles the situation is clear: with so few constraints, lens models are unable to recognize and constrain an environmental contribution to the lens potential; to fix the errors, it will be necessary to study the environment separately and impose it on the lens models.

For quads, lens models are often able to constrain shear from the environment, but the shear approximation clearly fails to capture all of the environmental effects. Returning to equation (5), the question is whether the errors are caused mainly by neglect of the convergence term (κ_{env}, representing the additional mass at the position of the lens galaxy) or by neglect of the higher order terms. To address this question, we consider what would happen if we somehow knew κ_{env} for each galaxy and could include it in the models. According to the mass-sheet degeneracy (Gorenstein et al. 1988; Saha 2000), the κ_{env} term simply rescales some of the model quantities without affecting the goodness of fit; some of the key rescalings are

$$b \propto (1 - \kappa_{env}), \tag{18}$$

$$\sigma \propto (1 - \kappa_{env})^{1/2}, \tag{19}$$

$$h \propto (1 - \kappa_{env}), \tag{20}$$

$$\mu \propto (1 - \kappa_{env})^{-2}, \tag{21}$$

$$\tilde{\sigma} \propto (1 - \kappa_{env})^{-2(\nu-1)}, \tag{22}$$

where σ is the inferred velocity dispersion, while $\tilde{\sigma}$ is the biased cross section and ν is the power-law index of the source number counts (see § 3). Figures 12 and 13 show that this rescaling makes the model results much more accurate. In particular, it removes the *biases* in quantities such as the ellipticity, Hubble parameter, lens galaxy velocity dispersion, image magnifications, and Ω_Λ. There are still some random errors: 0.07 in e and h; and 0.20 and 0.16 in $\ln \mu$ (for the bright saddle and bright minimum images, respectively).[10] Interestingly, adding the convergence does not fix the underestimated quad/double ratio, because it rescales the two- and four-image cross sections in the same way, leaving the ratio unchanged. *Still, it appears that neglecting the convergence from the environment is the primary cause of the biases in lensing results for quads.* Whether the residual scatter is due to neglect of the higher order terms in equation (5) or just to observational noise is not clear from this analysis.

The problem is that the convergence is not directly observable, because it usually represents dark matter. Nor is there a reliable way to estimate the convergence from properties of lens models. This statement may seem surprising, because for simple environments dominated by a single spherical halo there is a general relation between shear—which can be inferred from lens models, at least for quads—and convergence (Miralda-Escudé 1991; Kaiser 1995):

$$\gamma_{env} = \langle \kappa_{env} \rangle_R - \kappa_{env}, \tag{23}$$

---

[10] These are the numbers for quads in which the lens models provide an acceptable fit (Fig. 12, *shaded histograms*).
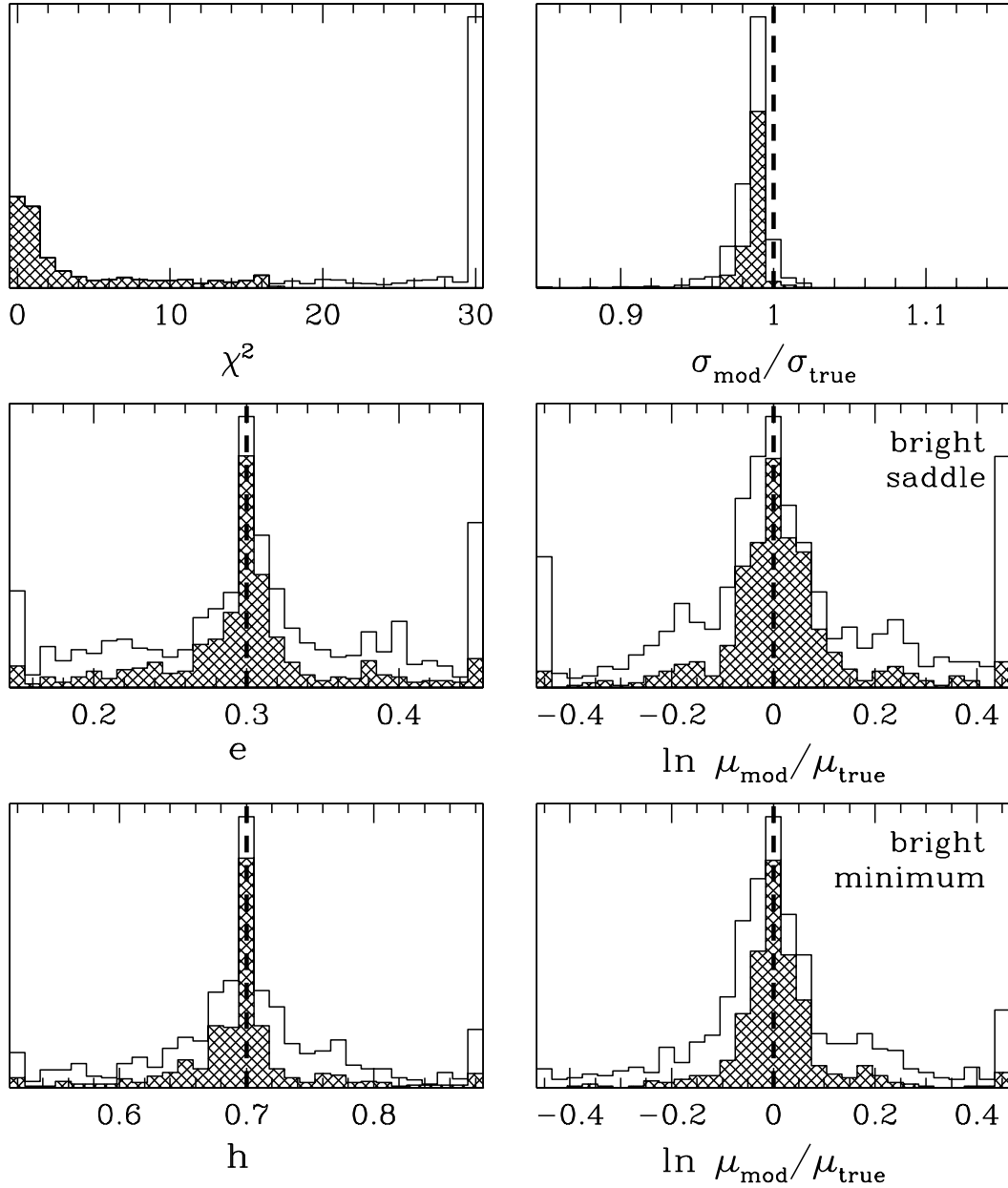
Fig. 12.—Sample results for mock quad lenses, for SIE+shear models that also include the convergence κ_{env} from the environment. We show histograms of the goodness of fit χ^2, the ellipticity, and the Hubble parameter (*left*), as well as errors in the lens galaxy velocity dispersion and the magnifications of the bright saddle and bright minimum images (*right*); this figure is to be compared with Figs. 4, 5, and 7 (but note the different axis scales). As before, the open histograms show all quads while the shaded histograms show those where the model provides an acceptable fit.

where R is the offset between the lens galaxy and the environment halo, and $\langle \kappa_{env} \rangle_R$ is the mean convergence (or surface mass density in units of the critical density for lensing) in an aperture of radius R centered on the environment halo. Because of the average, κ_{env} and γ_{env} depend on radius and on the halo properties (mass, concentration, etc.) in different ways, and there is no universal relation between them. A second and more troubling problem is that the convergence is a scalar while the shear is a rank-2 traceless tensor (or a headless vector with an amplitude and a direction that is invariant under $180°$ rotations; see eq. [5]). This means that in an environment comprising multiple mass components, the convergence and shear from the different components sum in different ways, and attempts to relate the net convergence to the net shear break down. A final problem is that this could

never work for doubles anyway, since there are no good model constraints on the shear.

The only solution is to build a model that allows us to translate observable quantities into reliable inferences about the convergence. If we can identify and model all of the mass components in the lens environment, then the shear, convergence, and higher order terms will all be included self-consistently. Creating such a model is not as crazy as it may sound, because many of the key parameters are observable. For example, the relative positions of the group member galaxies can be measured, and the relative magnitudes can be used to derive the b ratios (recall the Faber-Jackson relation, eq. [3]). Although the mass ellipticities cannot be directly observed, we can hypothesize that they are not critical; we can set them to zero when modeling the mock lenses and see
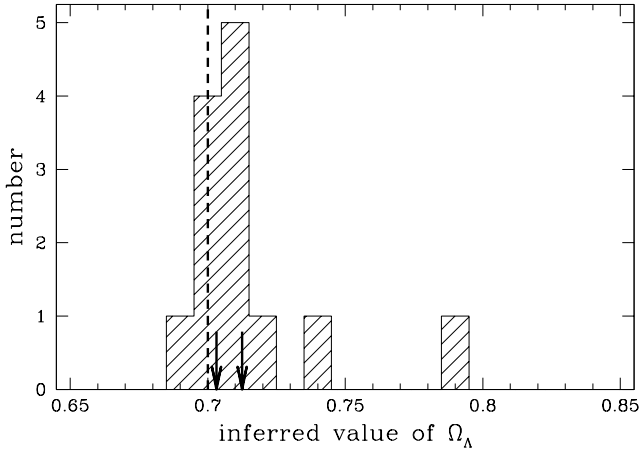
Fig. 13.—Similar to Fig. 10, but for SIE+shear models that also include the convergence κ_{env} from the environment. The dashed line shows the input value $\Omega_\Lambda = 0.7$. The arrow at $\Omega_\Lambda = 0.712$ shows the value if we average over the 13 galaxies (weighting each by its cross section). The arrow at $\Omega_\Lambda = 0.703$ shows the value if we assume that 25% of all lens galaxies lie in groups like our mock group, while the other 75% are isolated.

whether we still obtain accurate model results. (To be precise, we let the main lens galaxy be elliptical but make all the *other* galaxies circular.) In other words, all of the new parameters in the most basic *realistic* model of environment are either constrained by observations or fixed, so adding complexity has not caused an explosion of free parameters. We now consider whether such models are sufficient to fix the problems in lensing analyses. To allow for realistic noise in the observational constraints on the new parameters, we include generous uncertainties: measurement errors of $1''$ in the relative positions; and intrinsic scatter of 0.08 dex in the $\sigma(L)$ relation (Sheth et al. 2003), or 0.16 dex in the model b ratios.

Figure 14 shows the results when we apply such models to quad lenses. There are no biases in the results, and the scatter is encouragingly small: just 0.02 in both e and h; and 0.05–0.06 in $\ln\mu$. In other words, models that include the environment break the mass-sheet degeneracy and fix the problems with standard lensing analyses. Furthermore, these models do notably better than the models in Figures 12 and 13 that just included convergence, indicating that the higher order terms in the lens potential from the environment (eq. [5]) are in fact significant. Note that neither the assumption of circular group galaxies nor the inclusion of noise causes significant problems in the models.

Figure 15 shows that similar results hold for doubles, with slightly larger scatter: 0.07 in e; 0.03 in h; and 0.08 in $\ln\mu$. While we saw in § 4 that doubles are largely useless for astrophysical measurements when environments are unknown, we see now that observing and modeling the environment makes doubles almost as valuable as quads. Finally, Figures 16 and 17 show that Ω_Λ and the quad/double ratio can also be recovered well from statistical models that account for environment.

6. DISCUSSION

In this paper we have effectively studied 13 different galaxy/environment configurations, but they were all drawn from a single mock group of galaxies. We must therefore acknowledge the following caveats and questions about our results.

Is our mock group realistic? We constructed the system to mimic the group around the observed four-image lens PG 1115+080, and to be similar to nearby X-ray luminous groups, so it has reasonable properties. Furthermore, the distribution of lensing shears produced by the system is similar to what is measured and predicted for (quad) lenses (see Holder & Schechter 2003), so the group's contribution to the lens potential seems realistic. However, the proper way to answer this question is to study more real groups around real lenses in detail.

Is this group typical? Our group represents just one sample system. Based on current knowledge of lens environments (limited though it is) and on the shear distribution, we believe that it captures features that are representative. But we must identify the full distribution of lens environments before we can say for sure.

How do the results depend on the group properties? It seems likely that the systematic effects will scale with the mass or richness of the environment. However, that glib generalization obscures a lot of interesting details. A group's contribution to the lens potential may depend on many properties beyond its total mass: the ellipticities of the group member galaxies (addressed briefly in this paper); the properties of the galaxy population, such as the elliptical/spiral and dwarf/giant ratios; the fraction of mass in the common halo versus that bound to the galaxies (e.g., the degree to which the galaxy halos have been truncated by tidal stripping); the radial profile and angular structure of the common halo; and the offset between the group centroid and the lens galaxy. In the limit that the environment is dominated by a common dark halo, we must also understand how well observables such as the group centroid and velocity dispersion will be able to constrain the important properties of the environment. Studying these issues in detail is the subject of the follow-up paper.

Much more detailed understanding of lens environments is clearly required. We need to characterize the distribution of lens environments in order to guide theoretical calculations. For lenses lying in groups (or clusters), we must find the member galaxies and measure the centroid and velocity dispersion of the system and then build sophisticated lens models that finally treat environments properly. Even for lenses that do not lie in groups or clusters, careful observations will be needed in order to establish that the environments are unimportant.

7. CONCLUSIONS

Poor groups of galaxies around strong gravitational lens systems can affect lensing constraints on the masses and shapes of galaxy dark matter halos, the amount of substructure in dark matter halos, the quad/double ratio, the properties of lensed sources, the Hubble constant, and the dark energy density. Not knowing that a lens lies in a group can cause biases and uncertainties in lensing analyses. Models of double lenses that neglect the environment will generally fit the data well ($\chi^2 \approx 0$) but yield parameter values that are grossly incorrect. Models of quad lenses will reveal that environment cannot be ignored but will not fully constrain the environmental component of the lens potential. The standard shear approximation for quads is generally adequate for fitting the data, but not for recovering correct parameter values. The essential point is that the environment-related errors are not random errors but systematic biases, such as overestimates of
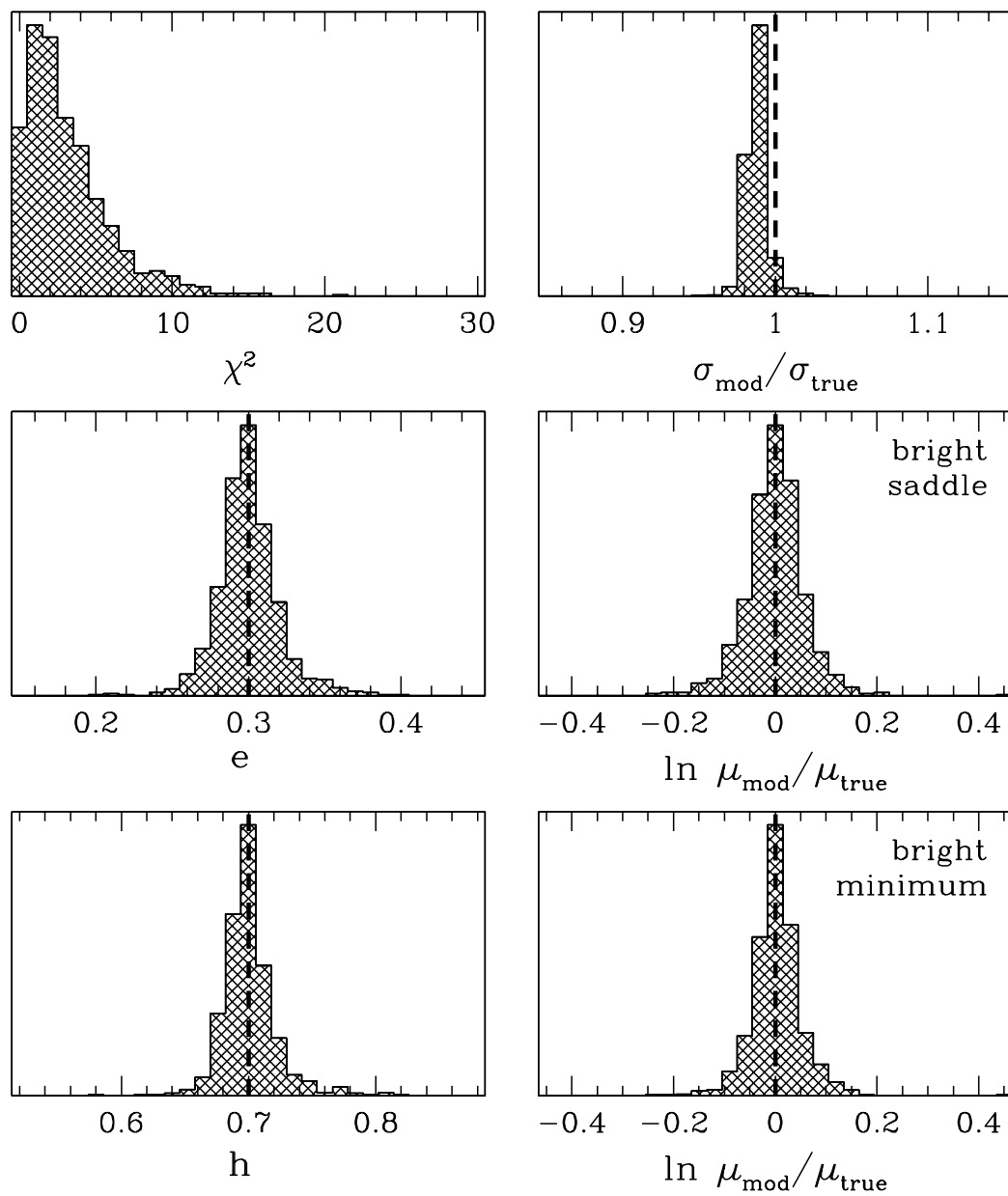
Fig. 14.—Similar to Fig. 12, but for models that incorporate all of the group member galaxies using reasonable observational constraints. Here all of the quads are well fitted by the models.
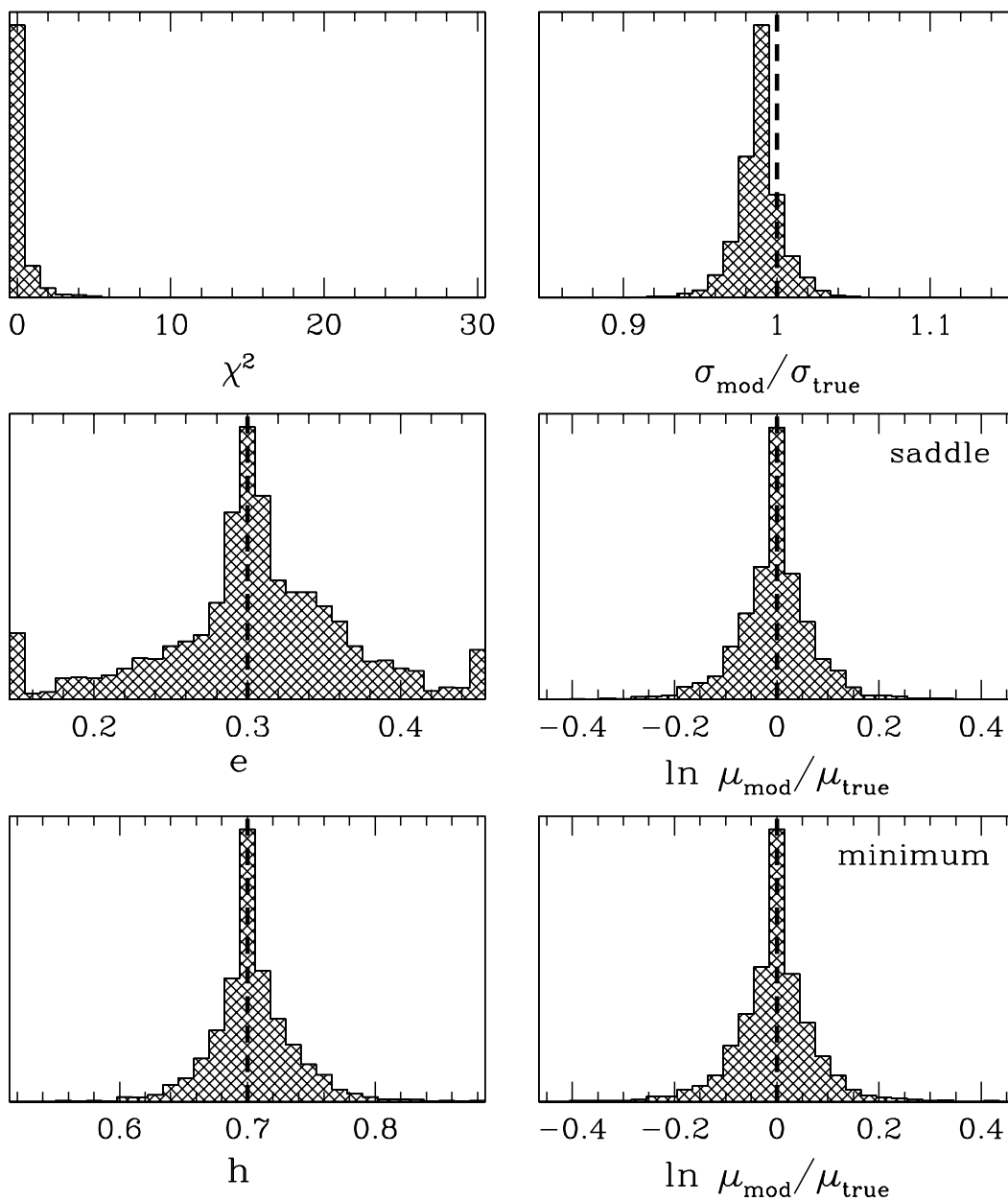
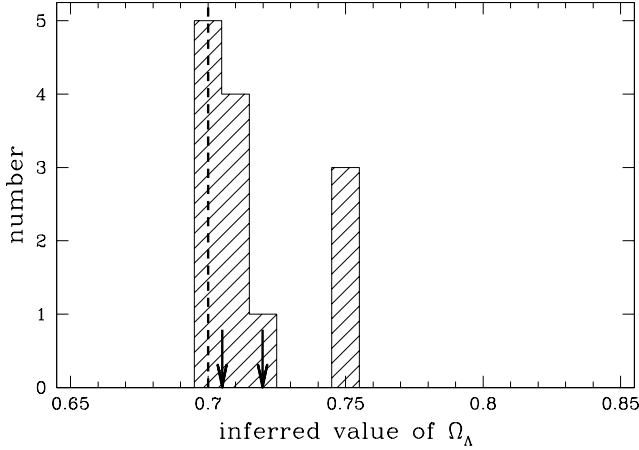Fig. 15.—Similar to Fig. 14, but for mock double lenses.

Fig. 16.—Similar to Fig. 13, but for models that incorporate the group member galaxies using reasonable observational constraints. The arrow at $\Omega_\Lambda = 0.720$ shows the value if we average over the 13 galaxies (weighting each by its cross section). The arrow at $\Omega_\Lambda = 0.705$ shows the value if we assume that 25% of all lens galaxies lie in groups like our mock group, while the other 75% are isolated.
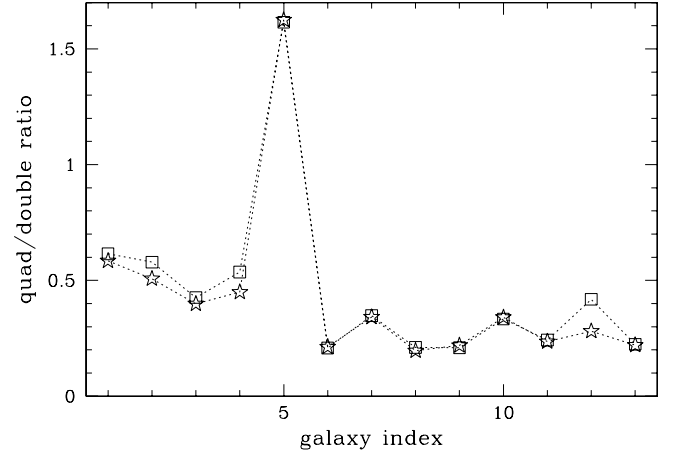

Fig. 17.—Similar to Fig. 11, but for models that incorporate the group member galaxies. The squares again show the quad/double ratios when the galaxies are placed in their true environments, while the stars show the values using the model environments. The net ratio with the model environments is 0.45 compared with the true value of 0.50.

lens galaxy velocity dispersions, the Hubble constant, and Ω_Λ, and underestimates of the image magnifications.

These systematic effects help resolve one long-standing puzzle in lensing but seem to aggravate two others. The solved problem is the high number of quad lenses relative to doubles (also see Cohn & Kochanek 2004). We have shown that neglecting environment can cause models to significantly underestimate the quad/double ratio; accounting for environment can increase the ratio to near the observed value.

The first unsolved problem involves lensing and the Hubble constant. Analyses of lens time delays that invoke what we think we know about galaxy dark matter halos yield $H_0 \sim 50$ km s^{-1} Mpc^{-1}, which is low compared with the conventional value $H_0 \sim 70$ (see Kochanek 2002, 2003, and references therein). We find that poor knowledge of environments causes an overestimate of H_0, so accounting for environment would *worsen* the problem. The extent of this problem is actually unclear, because some other lensing analyses yield $H_0 \sim 70$ (e.g., Koopmans et al. 2003; Saha & Williams 2004). In any case, there is a discrepancy remaining to be resolved, and the role of environments cannot be ignored.

The second puzzle involves lensing constraints on Ω_Λ. Traditional lensing analyses have tended to produce low values of Ω_Λ, such as the oft-quoted bound $\Omega_\Lambda < 0.66$ at 95% confidence (Kochanek 1996a), that are in marginal conflict with the concordance cosmology. We find that poor knowledge of environments leads to an overestimate of Ω_Λ, which would seem to worsen the problem. However, updated analyses have revised the lensing results upward, with best-fit values in the range $\Omega_\Lambda \approx 0.72$–$0.78$ (Mitchell et al. 2004). In this case, correcting for environment might even resolve any discrepancies that may remain between lensing and other methods.

Apart from a general desire to make lensing analyses accurate, there is new impetus to control the systematics. Linder (2004) recently pointed out that if lens models can be made accurate at the $\sim 1\%$ level then strong lensing can probe the dark energy equation of state in a manner complementary to the other probes now being discussed (such as supernovae, the microwave background, and weak lensing). We have argued that as long as lens environments are poorly understood there is no way for lensing to achieve this kind of accuracy. But if environments receive the kind of detailed study they deserve, the prospects are good for lensing to participate in the new era of precision cosmology.

REFERENCES

Bartelmann, M., & Schneider, P. 2001, Phys. Rep., 340, 291
Bender, R., Surma, P., Döbereiner, S., Möllenhoff, C., & Madejski, R. 1989, A&A, 217, 35
Bernstein, G., & Fischer, P. 1999, AJ, 118, 14
Browne, I. W. A., et al. 2003, MNRAS, 341, 13
Burud, I., et al. 2002a, A&A, 383, 71
———. 2002b, A&A, 391, 481
Chae, K.-H. 2003, MNRAS, 346, 746
Chae, K.-H., & Mao, S. 2003, ApJ, 599, L61
Chang, K., & Refsdal, S. 1979, Nature, 282, 561
Chiba, M. 2002, ApJ, 565, 17
Cohn, J. D., & Kochanek, C. S. 2004, ApJ, 608, 25
Colley, W. N., et al. 2003, ApJ, 587, 71

Dalal, N., & Kochanek, C. S. 2002, ApJ, 572, 25
Fabbiano, G. 1989, ARA&A, 27, 87
Fassnacht, C. D., & Lubin, L. M. 2002, AJ, 123, 627
Fassnacht, C. D., Xanthopoulos, E., Koopmans, L. V. E., & Rusin, D. 2002, ApJ, 581, 823
Franx, M. 1993, in IAU Symp. 153, Galactic Bulges, ed. H. DeJonghe & H. J. Habing (Dordrecht: Kluwer), 243
Gerhard, O., Kronawitter, A., Saglia, R. P., & Bender, R. 2001, AJ, 121, 1936
Gladders, M. D., Hoekstra, H., Yee, H. K. C., Hall, P. B., & Barrientos, L. F. 2003, ApJ, 593, 48
Gorenstein, M. V., Shapiro, I. I., & Falco, E. E. 1988, ApJ, 327, 693
Gott, J. R. 1977, ARA&A, 15, 235

Grant, C. E., Bautz, M. W., Chartas, G., & Garmire, G. P. 2003, preprint (astro-ph/0305137)

Holder, G., & Schechter, P. 2003, ApJ, 589, 688

Im, M., et al. 2002, ApJ, 571, 136

Impey, C. D., Falco, E. E., Kochanek, C. S., Lehár, J., McLeod, B. A., Rix, H.-W., Peng, C. Y., & Keeton, C. R. 1998, ApJ, 509, 551

Inada, N., et al. 2003, Nature, 426, 810

Jørgensen, I., Franx, M., & Kjaergaard, P. 1995, MNRAS, 273, 1097

Kaiser, N. 1995, ApJ, 439, L1

Kassiola, A., & Kovner, I. 1993, ApJ, 417, 459

Keeton, C. R. 2001, preprint (astro-ph/0102340)

———. 2003, ApJ, 584, 664

Keeton, C. R., Christlein, D., & Zabludoff, A. I. 2000, ApJ, 545, 129

Keeton, C. R., & Kochanek, C. S. 1997, ApJ, 487, 42

———. 1998, ApJ, 495, 157

Keeton, C. R., Kochanek, C. S., & Falco, E. E. 1998, ApJ, 509, 561

Keeton, C. R., Kochanek, C. S., & Seljak, U. 1997, ApJ, 482, 604

Keeton, C. R., & Winn, J. 2003, ApJ, 590, 39

King, L. J., Browne, I. W. A., Wilkinson, P. N., & Patnaik, A. R. 1996, in Astrophysics Applications of Gravitational Lensing, ed. C. S. Kochanek & J. N. Hewitt (Dordrecht: Kluwer), 191

Kneib, J.-P., Cohen, J. G., & Hjorth, J. 2000, ApJ, 544, L35

Kochanek, C. S. 1991, ApJ, 373, 354

———. 1993a, MNRAS, 261, 453

———. 1993b, ApJ, 419, 12

———. 1994, ApJ, 436, 56

———. 1996a, ApJ, 466, 638

———. 1996b, ApJ, 473, 595

———. 2002, ApJ, 578, 25

———. 2003, ApJ, 583, 49

Kochanek, C. S., & Dalal, N. 2003, preprint (astro-ph/0302036)

Kochanek, C. S., Keeton, C. R., & McLeod, B. A. 2001, ApJ, 547, 50

Kochanek, C. S., & Schechter, P. L. 2003, in Measuring and Modeling the Universe, ed. W. L. Freedman (Carnegie Obs. Astrophys. Ser. Vol. 2; Cambridge: Cambridge Univ. Press)

Koopmans, L. V. E., Garrett, M. A., Blandford, R. D., Lawrence, C. R., Patnaik, A. R., & Porcas, R. W. 2002, MNRAS, 334, 39

Koopmans, L. V. E., Treu, T., Fassnacht, C. D., Blandford, R. D., & Surpi, G. 2003, ApJ, 599, 70

Kormann, R., Schneider, P., & Bartelmann, M. 1994, A&A, 284, 285

Kuhlen, M., Keeton, C. R., & Madau, P. 2004, ApJ, 601, 104

Kundić, T., Cohen, J. G., Blandford, R. D., & Lubin, L. M. 1997a, AJ, 114, 507

Kundić, T., Hogg, D. W., Blandford, R. D., Cohen, J. G., Lubin, L. M., & Larkin, J. E. 1997b, AJ, 114, 2276

Lehár, J., et al. 2000, ApJ, 536, 584

Linder, E. V. 2004, preprint (astro-ph/0401433)

Mao, S., & Schneider, P. 1998, MNRAS, 295, 587

Marlow, D. R., et al. 2000, AJ, 119, 2629

McKay, T. A., et al. 2002, ApJ, 571, L85

Metcalf, R. B., & Madau, P. 2001, ApJ, 563, 9

Metcalf, R. B., Moustakas, L. A., Bunker, A. J., & Parry, I. R. 2004, ApJ, 607, 43

Miralda-Escudé, J. 1991, ApJ, 370, 1

Mitchell, J. L., Keeton, C. R., Frieman, J. A., & Sheth, R. K. 2004, preprint (astro-ph/0401138)

Mulchaey, J. S., & Zabludoff, A. I. 1998, ApJ, 496, 73

Nemiroff, R. J. 1988, ApJ, 335, 593

Ofek, E. O., Rix, H.-W., & Maoz, D. 2003, MNRAS, 343, 639

Paczyński, B. 1986, ApJ, 301, 503

Patnaik, A. R., Kemball, A. J., Porcas, R. W., & Garrett, M. A. 1999, MNRAS, 307, L1

Peng, C. Y., et al. 2004, ApJ, submitted

Refsdal, S. 1964, MNRAS, 128, 307

Richards, G. T., et al. 2004, ApJ, 610, 679

Rix, H.-W., de Zeeuw, P. T., Carollo, C. M., Cretton, N., & van der Marel, R. P. 1997, ApJ, 488, 702

Rix, H.-W., Falco, E., Impey, C., Kochanek, C., Lehár, J., McLeod, B., Muñoz, J., & Peng, C. 2001, in ASP Conf. Ser. 237, Gravitational Lensing: Recent Progress and Future Goals, ed. T. Brainerd & C. Kochanek (San Francsico: ASP), 169

Romanowsky, A., et al. 2003, Science, 301, 1696

Saglia, R. P., Bender, R., & Dressler, A. 1993, A&A, 279, 75

Rusin, D., & Tegmark, M. 2001, ApJ, 553, 709

Rusin, D., et al. 2001, ApJ, 557, 594

———. 2003a, ApJ, 587, 143

Rusin, D., Kochanek, C. S., & Keeton, C. R. 2003b, ApJ, 595, 29

Saha, P. 2000, AJ, 120, 1654

Saha, P., & Williams, L. L. R. 1997, MNRAS, 292, 148

———. 2003, AJ, 125, 2769

———. 2004, AJ, 127, 2604

Schade, D., et al. 1999, ApJ, 525, 31

Schechter, P. L., et al. 1997, ApJ, 475, L85

Schechter, P. L., & Wambsganss, J. 2002, ApJ, 580, 685

Schmidt, R., & Wambsganss, J. 1998, A&A, 335, 379

Schneider, P., Ehlers, J., & Falco, E. E. 1992, Gravitational Lenses (Berlin: Springer)

Sheldon, E. S., et al. 2004, AJ, 127, 2544

Sheth, R. K., et al. 2003, ApJ, 594, 225

Tonry, J. L. 1998, AJ, 115, 1

Tonry, J. L., & Kochanek, C. S. 1999, AJ, 117, 2034

Treu, T., & Koopmans, L. V. E. 2002a, ApJ, 575, 87

———. 2002b, MNRAS, 337, L6

———. 2004, preprint (astro-ph/0401373)

Trotter, C. S., Winn, J. N., & Hewitt, J. N. 2000, ApJ, 535, 671

Turner, E. L. 1990, ApJ, 365, L43

Turner, E. L., Ostriker, J. P., & Gott, J. R. 1984, ApJ, 284, 1

van Waerbeke, L., & Mellier, Y. 2003, preprint (astro-ph/0305089)

Wyithe, J. S. B., Webster, R. L., & Turner, E. L. 2000, MNRAS, 315, 51

Young, P., Gunn, J. E., Oke, J. B., Westphal, J. A., & Kristian, J. 1980, ApJ, 241, 507

Zabludoff, A. I., & Mulchaey, J. S. 1998, ApJ, 496, 39

———. 2000, ApJ, 539, 136

Zaritsky, D., & Gonzalez, A. H. 2003, ApJ, 584, 691

Zaritsky, D., & White, S. D. M. 1994, ApJ, 435, 599

Zhao, H., & Pronk, D. 2001, MNRAS, 320, 401